Unraveling immunomodulatory mechanism of mesenchymal stem cell derived secretome in mouse models of rheumatoid arthritis and systemic lupus erythematosus

Taejun Yoon

Department of Medical Science

The Graduate School, Yonsei University

Unraveling immunomodulatory mechanism of mesenchymal stem cell derived secretome in mouse models of rheumatoid arthritis and systemic lupus erythematosus

Directed by Professor Yong-Beom Park

The Doctoral Dissertation
submitted to the Department of Medical Science,
the Graduate School of Yonsei University
in partial fulfillment of the requirements for the degree of
Doctor of Philosophy in Medical Science

Taejun Yoon

December 2023

This certifies that the Doctoral Dissertation of
Taejun Yoon is approved.

Yong Beom Park

Thesis Supervisor : Yong-Beom Park

Thesis Committee Member#1 : Hyoung-Pyo Kim

Thesis Committee Member#2 : Jeon-Soo Shin

Thesis Committee Member#3: Sang-Won Lee

Thesis Committee Member#4: Je-Wook Yu

The Graduate School
Yonsei University

December 2023

ACKNOWLEDGEMENTS

I will give my huge thanks to many people who have been helped me during my term of PhD degree.

First, I really appreciate Yong-Beom Park for his generous support. He led me to become a great researcher with critical thinking and ability to make independent judgments about research.

I also would like to show my sincere thanks to members of my dissertation committee: Prof. Hyoung-Pyo Kim, Prof. Jeon-Soo Shin, Prof. Sang-Won Lee, and Prof. Je-Wook Yu for giving me continuous guidance and sharpening my thinking as an independent researcher.

I would like to thank Yonsei Rheuma lab members and many researchers who shared joy, anger, sorrow, and pleasure together.

Last but not least, I would like to express my gratitude to my family. My father and mother always give me both critical advice and sincere support. My parents in law also gave me huge support. Foremost, my wife hesitated at nothing to sacrifice everything to support me and my son give me vitality of my life.

I am still not a perfect researcher, but I will continue to improve myself as a good researcher with what I learned during my term of PhD degree.

All glory belongs to God and Thank you.

Dec 2023

Taejun Yoon

TABLE OF CONTENTS

LIST OF FIGURES

LIST OF TABLES

ABSTRACT

Unraveling immunomodulatory mechanisms of mesenchymal stem cell derived secretomes in mouse models of rheumatoid arthritis and systemic lupus erythematosus

Taejun Yoon

Department of Medical Science

The Graduate School, Yonsei University

(Directed by Professor Yong-Beom Park)

Mesenchymal stem cells (MSCs) exert immunomodulatory and anti-inflammatory effect to several diseases and immune cells, but they have several limitations as a therapeutic agent. Secretome, secreted bioactive molecules, derived from MSCs is proposed as an alternative to overcome the limitations. Among several diseases, autoimmune diseases, result from the defect in immune system, are one of the targets for applying MSCs as a new treatment to cover present unmet needs. Macrophages have function in homeostasis with regulating immune systems and express two functional

phenotypes, classically activated M1 and alternatively activated M2 macrophages. Recently, the importance of M2 subtypes, M2a, M2b, M2c, and M2d, is emerging to understand detailed mechanisms of macrophages. Several recent studies tried to clarify therapeutic efficacy and its mechanisms of MSCs; however, it is not fully understood. In this study, the therapeutic efficacy of MSCs derived secretome was observed and the underlying mechanism was studied with searching materials of immune modulation from secretome.

For in vitro assay, a macrophage cell line, RAW264.7 cells and mouse peritoneal macrophages were treated with adipose derived MSC (ADSC) secretome in the absence or presence of LPS stimulation. Pro-inflammatory markers and anti-inflammatory markers of macrophages were analyzed with flow cytometry (FACS), qRT-PCR, and enzyme-linked immunosorbent assay (ELISA). To identify the mechanism of ADSC secretome, NF-κB/AKT and STAT/SOCS pathways of macrophage were observed by western blot. Therapeutic efficacy of ADSC secretome was confirmed with animal models of rheumatoid arthritis, collagen induced arthritis (CIA) and of systemic lupus erythematosus (SLE), NZB W/F1 mouse. ADSC secretome was analyzed by LC/MS-MS proteomics and DAVID bioinformatics. Antibody neutralization and recombinant protein were used to confirm pivotal molecules in ADSC secretome.

ADSC secretome suppressed pro-inflammatory markers such as iNOS and TNF-α and enhanced anti-inflammatory markers such as Arg-1 and IL-10 of macrophages. ADSC secretome also suppressed phosphorylation of NF-κB and AKT with the increase of PTEN

expression of macrophages. Also, a PTEN inhibitor diminished the immune-modulatory effect of ADSC secretome. Phosphorylation of STAT1 was reduced and of STAT3 was escalated with activation of SOCS1 and SOCS3 by ADSC secretome. ADSC secretome alleviated disease activity of CIA and NZB/W F1 mouse and made peritoneal macrophages express M2b/c-like phenotype. From the proteomics analysis, 84 proteins were discovered in ADSC secretome and 7 candidate molecules (ANAX1, CFH, DKK3, LGALS3BP, PTX3, PROS1, and SERPINF1) were selected. Among them, pentraxin-3 (PTX3) was chosen for the further examination. Antibody neutralization of PTX3 reduced the function of ADSC secretome and recombinant PTX3 showed similar effect with ADSC secretome.

ADSC secretome regulated inflammation in RAW264.7 cells and animal models of RA and SLE. Also, ADSC secretome was involved in M2b/c polarization of peritoneal macrophage and PTX3 is a key molecule of the effect.

Key words : mesenchymal stem cell, secretome, macrophages, autoimmune diseases, immunomodulation

Unraveling immunomodulatory mechanisms of mesenchymal stem cell derived secretomes in mouse models of rheumatoid arthritis and systemic lupus erythematosus

Taejun Yoon

Department of Medical Science

The Graduate School, Yonsei University

(Directed by Professor Yong-Beom Park)

I. INTRODUCTION

Mesenchymal stem cells (MSCs) are multipotent stem cells, which possess the ability to differentiate to various cell types, characterized by self-renewal ability.[1] Based on various origins of MSCs such as bone marrow, adipose tissue, and umbilical cord, MSCs can be acquired easily compared to the other stem cells.[2] Also, MSCs are less affected by ethical limitation than other stem cells.[3] Nevertheless, MSCs cell therapy still has huddles

to use in clinic such as shortage of standardization of managing cells and delivery route, function loss during the cell expansion, and adverse effects.[4,5] MSCs exert their therapeutic efficacy through several mechanisms other than cell-cell interaction: paracrine activity, transfer of organelles and molecules by through tunneling nanotubes, and exosomes or microvesicles.[6] Especially, MSCs express immunomodulatory and anti-inflammatory effect by secreting several bioactive molecules containing secreted proteins (secretome).[7,8]

Autoimmune diseases occur with malfunction of immune system, recognition own body as foreign object and attacking it because of abnormal activation. These diseases are related to chronic inflammation in several tissues and collapse of immune homeostasis.[9] Current treatments for autoimmune diseases focus on suppressing immune function to modify inflammation but they have several limitations such as incomplete treatment responses and increased vulnerability of infection.[10] As MSCs have immunosuppressive and regenerative properties, MSCs are suggested as an alternative treatment to overcome the current limitations and several studies reported that MSCs have therapeutic efficacy to autoimmune diseases, such as systemic lupus erythematosus (SLE), multiple sclerosis (MS), and rheumatoid arthritis (RA).[11-14]

Macrophages play a vital role in the innate and acquired immune systems. Well known functions of macrophage are host defense and apoptotic cells removal for tissue homeostasis and immunoregulating.[15] Macrophages also have diversity and plasticity as their characteristics. Under functional plasticity, macrophages polarize between two functional phenotypes, classically activated M1 and alternatively activated M2

macrophages according to the specific condition.[16] M1 macrophages can be induced by IFN-γ or LPS and as they have ability to remove pathogen effectively, they secrete inflammatory cytokine and produce nitric oxide (NO). IL-4 and IL-13 are popular inducers of M2 macrophages, which carry out pathogen defense with improved phagocytosis. Conversely to M1 macrophages, M2 macrophages induce anti-inflammatory condition and are involved in would healing and tissue repair with secreting high levels of TGF-β1 and IL-10.[17-19] M2 macrophages are further classified as M2a, M2b, M2c, and M2d subtypes according to each stimulants and each subtype has different characteristics in exhibiting immune-modulatory ability.[20,21] Recently, significance in investigating impact of M2 subtypes on mechanism of diseases were proposed in many studies.[22-25] Especially, Alivernini et al. addressed that the number of MerTK+ macrophages, M2c subtypes, are short in synovial tissue of rheumatoid arthritis patients and related to the improvement of treatment.[26]

MSCs induce polarization of macrophage toward M2 state considered as having immune-modulation characteristics with increased expression of arginase-1 (Arg-1) and decreased inducible nitric oxide synthase (iNOS).[27] Furthermore, MSCs generate M2b/c like polarization with increased LIGHT (M2b) and MerTK (M2c) expressions of macrophages.[28,29] Also, several studies reveal PGE2, TSG-6, TGF-β1, and IL-6 as secreted molecules that exhibit immune-modulatory function of MSCs.[28,30-33] Even though notable attempts were established, MSCs derived secretome still needs to be investigated further to utilize as therapeutic agent. In this study, we examined the therapeutic efficacy of MSCs

derived secretome in animal models of RA and SLE and the mechanism of immunomodulatory effect and anti-inflammatory effect of the secretome with macrophages.

II. MATERIALS AND METHODS

1. Isolation of secretome from adipose tissue-derived MSCs

Adipose tissue-derived MSCs (ADSCs) were maintained with low glucose (1 g/L) Dulbecco's modified Eagle medium (DMEM, Corning, NY, USA) supplemented with 10% fetal bovine serum (FBS, Corning), 1% nonessential amino acids, and 1% penicillin–streptomycin at 37 °C in 5% CO_2. When the confluence became over 90% at passage 6, MSCs were cultured with FBS-free DMEM without phenol red containing 1% penicillin-streptomycin for 48 hr. The cultured medium is gathered, residue such as cell debris was removed by centrifugation at 2000 RPM for 5 min, and the secretome was isolated using a tangential flow filtration (TFF) capsule with 3 kDa molecular weight cut-off (MWCO) membrane (Pall Corporation, Ann Arbor, MI, USA). Protein concentrations of secretome were quantified by BCA assay (Thermo Fisher Scientific, Waltham, MA, USA) and then secretome was stored at -80 °C until use.

2. ADSC secretome treatment in RAW264.7 macrophage cells

RAW264.7 cells were purchased from Korea Cell Line Bank and maintained with high glucose (4.5 g/L) DMEM containing 10% FBS and 1% penicillin-streptomycin in 6-well plates. For further experiment, cells were cultured with secretome and 1 μg/ml LPS (Sigma-Aldrich, St. Louis, MO) for 24 hr. For PTEN inhibitor experiment, 2 μM SF1670 (Abcam, Cambridge, UK) was added with secretome treatment.

3. Isolation of peritoneal macrophages and treatment with ADSC Secretome

8 ml of ice-cold PBS containing 3% FBS was injected into a peritoneal cavity of mouse and the peritoneum was gently massaged. The peritoneal fluid was collected and centrifuged at 1500 RPM for 5 min to collect peritoneal cavity cells. Cells were suspended with RPMI 1640 medium (Corning) containing 10% FBS, 20 mM HEPES, 1 mM sodium pyruvate, 100 U/ml penicillin, 100 μg/ml streptomycin, 0.1 mM non-essential amino acids, 20 μg/ml gentamycin, and 500 μM β-mercaptoethanol. Macrophages were plated as 1×10^6 cells/well in 6-well plates and incubated at 37 °C for 2 hr. Suspended cells were removed by gently washing with PBS. Adherent cells were cultured with treatment of secretome for 18 hr and stimulated with LPS for 4 hr before harvesting for further study.

4. Cell counting kit (CCK)-8 assay

RAW264.7 and peritoneal macrophages were plated in 96-well plates. After secretome treatment for 24 hr, 10 ul of CCK-8 solution (Sigma-Aldrich) was added to each well and incubated for 4 hr. Then, absorbance was measured at 450 nm by microplate reader, VersaMax (Molecular Device, Sunnyvale, CA, USA).

5. Flow cytometry analysis (FACS)

Harvested macrophages were washed by PBS with 1% FBS. Then, the cells were stained with F4/80-FITC, CD86-PE, CD206-APC (BD Biosciences, Oxford, UK),

AF700-LIGHT (R&D systems, Minneapolis, MN, USA), BV421-MerTK, and PerCP-Cy5.5-CD197 (Biolegend, San Diego, CA, USA). The cells were analyzed using a FACSVerse and FlowJo software (BD Biosciences).

6. Enzyme-linked immunosorbent assay (ELISA)

Supernatants from cultured macrophages were used for the cytokine measurement. Inflammatory cytokines, TNF-α, IL-6 (BD Biosciences), and IL-1β (Invitrogen, Carlsbad, CA, USA) and anti-inflammatory cytokine, IL-10 (BD Biosciences) were measured using commercially available ELISA kits according to the manufacturer's instruction.

7. Quantitative real time-polymerase chain reaction (qRT-PCR)

Total RNA of macrophages was extracted using a GeneJET RNA Purification Kit (Thermo Fisher Scientific) and cDNA was synthesized by Maxime RT PreMix (iNtRON Biotechnology, Seongnam, South Korea). Real-time PCR was performed using an AB Applied Biosystems platform with qPCR BIO Screen Mix Hi-ROX (PCR Biosystems, London, UK). mRNA expressions were determined with 40 μg of cDNA using an ABI Systems 7500 Fast Real-Time PCR System (Applied Biosystems, Weiterstadt, Germany). Primers used for the experiment were shown in Table 1.

Table 1. Primers for qRT-PCR

Genes	Forward	Reverse
iNOS	CCC TTC AAT GGT TGG TAC ATG G	ACA TTG ATC TCC GTG ACA GCC
TNF-α	TCT TCT CAT TCC TGC TTG TGG	GGT CTG GGC CAT AGA ACT GA
IL-6	GGA GCC CAC CAA GAA CGA TAG	GTG AAG TAG GGA AGG CCG TG
IL-1β	ATG GCA ACT GTT CCT GAA CTC AAC T	TTT CCT TTC TTA GAT ATG GAC AGG AC
IL-12p40	ATG GCC ATG TGG GAG CTG GAG AAA G	GTG GAG CAG CAG ATG TGA GTG GCT
CD86	TTG TGT GTG TTC TGG AAA CGG AG	AAC TTA GAG GCT GTG TTG CTG GG
COX-2	ATG CTC CTG CTT GAG TAT GT	CAC TAC ATC CTG ACC CAC TT
PGES1	GGA TGC GCT GAA ACG TGG A	CAG GAA TGA GTA CAC GAA GCC
Arg-1	GAA CAC GGC AGT GGC TTT AAC	TGC TTA GCT CTG TCT GCT TTG C
IL-10	AAT AAG AGC AAG GCA GTG	CCA GCA GAC TCA ATA CAC
CD206	TCT TTG CCT TTC CCA GTC TCC	TGA CAC CCA GCG GAA TTT C
TGF-β1	AGC AGT GCC CGA ACC CCC AT	GGG GTC AGC AGC CGG TTA CC
Ym-1	CAC CAT GGC CAA GCT CAT TCT TGT	TAT TGG CCT GTC CTT AGC CCA ACT
SPHK1	ACA GCA GTG TGC AGT TGA TGA	GGC AGT CAT GTC CGG TGA TG
LIGHT	CTG CAT CAA CGT CTT GGA GA	GAT ACG TCA AGC CCC TCA AG
MerTK	TCC TAC CTC CTG TTG CGT TT	ATT CAC ACT CTC AGG CTG CT
GAPDH	GTG TTC CTA CCC CCA ATG TGT	ATT GTC ATA CCA GGA AAT GAG CTT

8. Western blotting

Cells were lysed using RIPA buffer with a protease inhibitor and a phosphatase inhibitor. Concentrations of cell lysates were measured with BCA assay (Thermo Fisher Scientific). ~20 μg cell lysates were separated by sodium dodecyl sulfate polyacrylamide gel electrophoresis (SDS-PAGE, Bio-Rad, Hercules, CA, USA) and transferred onto a PVDF membrane (Sigma-Aldrich). The membrane was blocked with a commercial blocking solution (TransLab, Daejeon, South Korea) for 1 hr at room temperature. Then, incubation with primary antibodies was performed for 1 hr at room temperature or overnight at 4 ºC. After washing membranes, incubation with secondary antibody was performed for 1 hr at room temperature. Band intensities were visualized by West-Q PICO ECL solution (GenDEPOT, Katy, TX, USA) and ImageQuant 800 (GE Healthcare, Milwaukee, WI, USA). Relative expressions of the target proteins to β-actin or GAPDH are measured by Image Studio Lite software (LI-COR Biosciences, Lincoln, NE, USA). Used antibodies were listed as follows: iNOS (1:100, Abcam), Arg-1 (1:2000, BD Biosciences), pNF-κB, NF-κB, pAKT, AKT, PTEN, pSTAT1, STAT1, pSTAT3, STAT3, SOCS1, SOCS3 (1:1000, Cell Signaling Technology, Beverly, MA, USA), GAPDH, and β-actin (1:2000, Santa Cruz Biotechnology, Dallas, TX, USA).

9. Induction of collagen induced arthritis (CIA) and treatment with ADSC secretome

7 weeks old male DBA/1J mice (Central Lab Animal Inc., Seoul, Korea) were immunized by injecting 200 μg bovine type II collagen emulsified in Freund's complete adjuvant (1:1) containing 200 μg mycobacterium tuberculosis H37Ra intradermally at the base of the tail. After two weeks of the first immunization, the mice were immunized secondly by injecting 100 μg CII in incomplete Freund's adjuvant (1:1). All reagents for induction of CIA were purchased at Chondrex (Redmond, WA, USA)

Treatment was begun 52 days after the second immunization when the arthritis was well established. CIA mice were distributed randomly to three groups: Untreated CIA, MTX treatment, and secretome treatment. 35 mg/kg methotrexate (MTX) was injected intraperitoneally twice weekly to MTX treatment group. Secretome treatment group was injected with 10 mg/kg secretome intraperitoneally 3 times a week. The treatment lasted for 4 weeks.

10. Assessments of CIA

Mice were checked twice a week with observing clinical arthritis and weight. Clinical arthritis was scored on a scale of 0–4 (score 0 = no evidence of erythema and swelling, score 1 = erythema and mild swelling confined to the tarsal or ankle joint, score 2 = erythema and mild swelling extending from the ankle to the tarsal, score 3 = erythema and moderate swelling extending from the ankle to the metatarsal joints, and score 4 = erythema and severe swelling encompassing the ankle, foot, and digits or ankyloses of

the limb). The arthritis score of each animal was yield from summation of a grade of each paw. (maximum possible score, 16).

After 4 weeks of treatment, all mice were sacrificed and peritoneal macrophages and feet were collected to evaluate. Formalin fixed feet were decalcified in EDTA for 4 weeks and then embedded in paraffin. Embedded samples were cut into serial 4 μm sections and stained with hematoxylin and eosin (H&E). Sections were evaluated histopathologically and scored for inflammatory cell infiltration, synovial hyperplasia, and bone erosion, according to the criteria.[34]

11. Lupus-prone mouse (NZB/W F1) and treatment with ADSC secretome

21 weeks old female NZB/W F1 mice were obtained from Central Lab Animal Inc. and maintained at the Yonsei Laboratory Animal Research Center (YLARC, Seoul, Korea). Treatment was started at 23 weeks of age and lasted for 7 weeks. 7 mg/kg of methylprednisolone (MPL, Pfizer, Bruxelles, Belgium) and 10 mg/kg of secretome were injected intraperitoneally 3 times a week for MPL treatment and secretome treatment groups, respectively.

12. Assessments of NZB/W F1

Proteinuria and body weight were observed once a week for 7 weeks. Proteinuria was scored using protein reagent strips, URiSCAN (Yongdong Pharmaceutical Co., Yongin,

Korea) by the following scale: 0 = none or trace; 1 = ≤ 100 mg/dl; 2 = ≤ 300 mg/dl; 3 = ≤ 1,000 mg/dl; and 4 = ≥ 1,000 mg/dl.

All mice were sacrificed at 30 weeks of age and kidneys and peritoneal macrophages were acquired. Kidneys were fixed in formalin and then embedded in paraffin. Embedded specimens were cut into serial 4 μm sections and stained with H&E. Histopathological score was determined by the scoring system of renal damage as described previously: score 0 = no visible lesions, normal or near normal kidney morphology; score 1 = mild dilation in some tubules, cell swelling, luminal debris (cast), and nuclear condensation, partial loss of brush border membranes in < 1/3 tubules in high field; score 2 = obvious dilation of many tubules, loss of brush border membranes, nuclear loss, and cast in < 2/3 tubules in high field; score 3 = severe dilation of most tubules, total loss of brush border membranes, and nuclear loss in > 2/3 tubules in high field.[35]

13. Proteomic analysis

LC-MS/MS analysis with three secretome sets of three different donors was performed by ProteomeTech (Seoul, Korea). First, secretome sets were quantified with Bradford protein assay for the analysis. 2-DE electrophoresis was performed with 120 μg proteins for each sample and gels were stained with Coomassie brilliant blue G250. Spots were selected based on the image analysis using ImageJ and the selected spots were analyzed by LC/MS-MS method using nanoACQUITY UPLC and LTQ Orbitrap XL mass spectrometer (Thermo Fisher Scientific). Individual spectra from MS/MS were

processed by SEQUEST software (Thermo Quest, San Jose, CA, USA) and searched with NCBI database using MASCOT program (Matrix Sciences, London, UK.). Search parameters for data analysis were set as followed: Carbamidomethyl (C) as fixed modification, Deamidated (NQ) and Oxidation (M) as variable modifications, 10 ppm as tolerance of peptide mass, 0.8 Da as MS/MS ion mass tolerance, and 2 as allowance of missed cleavage. Peptides were selected with according to significance threshold in identity score of p values ≤ 0.05

14. Bioinformatics analysis

The Database for Annotation, Visualization and Integrated Discovery (DAVID) program was used for Gene Ontology (GO) enrichment analysis.[36] Identified protein list was uploaded to the functional annotation clustering tool. GO terms, which have the parameter of the FDR < 0.01 and p value < 0.05 were analyzed. p values were displayed as –Log10(p value).

15. Statistical analysis

All values represent the mean ± standard error of the mean (S.E.M.). The statistical significance of differences between two groups was compared using one-way ANOVA with a bonferroni post-test. Body weight change, mean arthritis score, and proteinuria were analyzed using two-way ANOVA test. p value ≤ 0.05 were considered significant. Statistical analyses were carried out using GraphPad Prism.

III. RESULTS

1. ADSC secretome suppresses inflammatory condition of LPS-stimulated RAW264.7 and induces M2 phenotypes

First, we showed that cell viability of RAW264.7 cells was not changed by ADSC secretome treatment below 100 μg/ml for 24 hr (Fig. 1A). RAW264.7 cells were stimulated with 1 μg/ml of LPS and treated with 100 μg/ml of ADSC secretome for 24 hr. Cells were stained with surface inflammatory markers, CD197 and CD86, and analyzed by flow cytometry. Expressions of both markers were increased in LPS group compared to control group and decreased in ADSC secretome group compared to LPS group (Fig. 1B). Then, pro-inflammatory cytokines (TNF-α and IL-1β) and anti-inflammatory cytokine (IL-10) were examined. TNF-α and IL-1β (Fig. 1C) were decreased and IL-10 (Fig. 1D) was increased in ADSC secretome group compared to LPS group. To verify the dose dependency of ADSC secretome, 10 μg/ml treatment groups was added and mRNA expressions were examined. mRNA levels of iNOS, TNF-α, and IL-6 were decreased and mRNA levels of Arg-1, IL-10, and CD206 were increased by ADSC secretome in dose dependent (Fig. 2A-B). Also, LPS-induced COX-2 and its related enzyme, mPGES1 were decreased by ADSC secretome in same manner with each other (Fig. 2C). Together, ADSC secretome controlled inflammatory activity of macrophages induced by LPS.

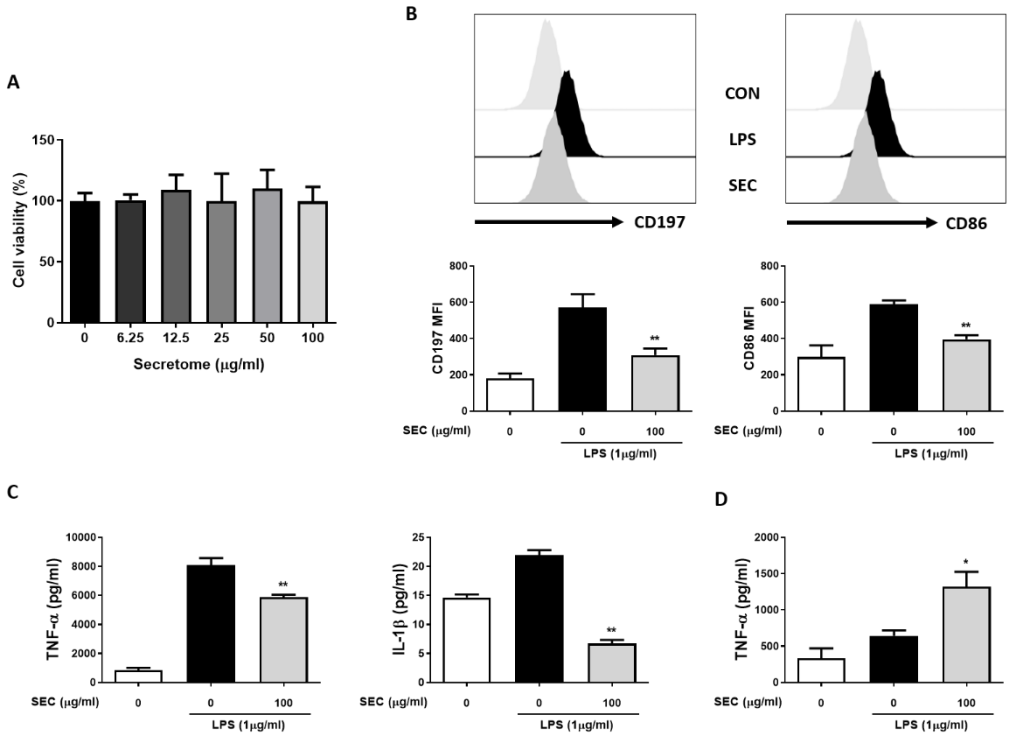

Figure 1. Establishing anti-inflammatory milieu of RAW264.7 cells by ADSC secretome. (A) Cell viability of RAW264.7 cells incubated for 24 hr with the ADSC secretome at various concentrations (B) Flow cytometry analysis of LPS (1 μg/ml)-activated RAW264.7 cells treated with or without 100 μg/ml ADSC secretome for 24 hr (C) Quantifications of TNF-α and IL-1β and (D) IL-10 in culture supernatant by ELISA. Data are expressed as mean ± SEM of four independent experiments. Statistical significance was determined by one-way ANOVA with a bonferroni post-test; $*P < 0.05$, $**P < 0.01$ compared to LPS-activated group. SEC: ADSC secretome; MFI: Mean fluorescent intensity.

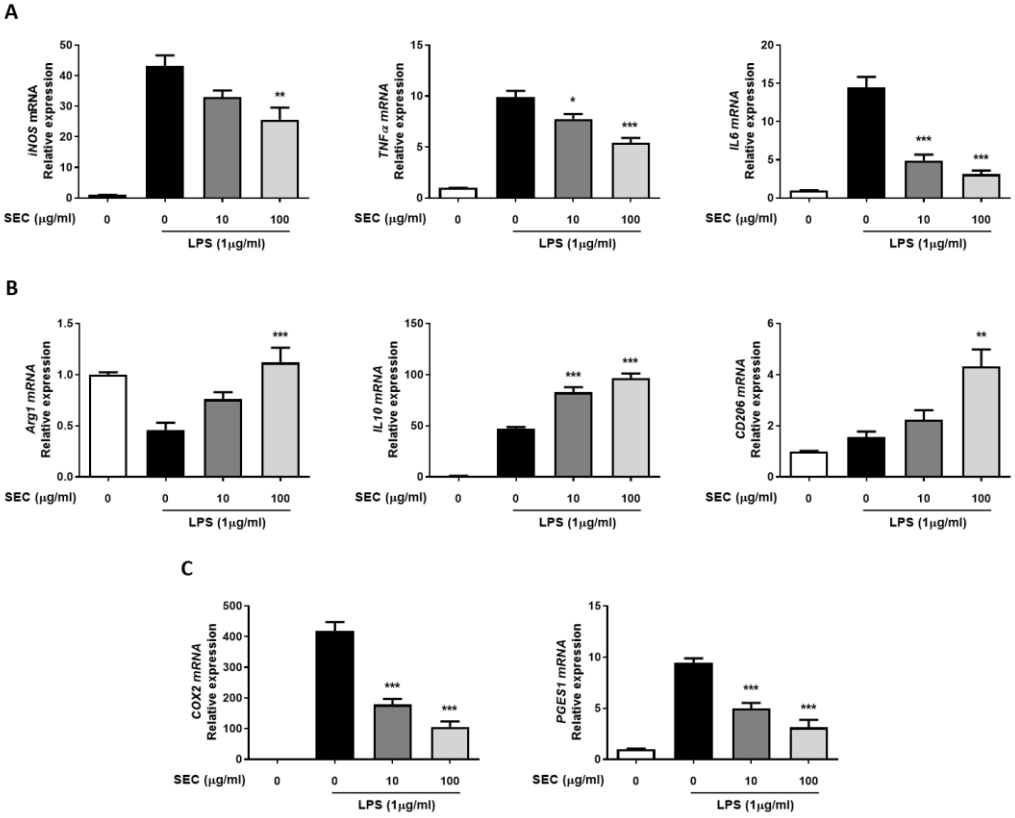

Figure 2. Change in gene expressions of RAW264.7 cells by ADSC secretome in concentration dependent manner. RAW264.7 cells were activated with 1 μg/ml LPS and treated with 10 or 100 μg/ml ADSC secretome for 24 hr. (A-C) Quantification of (A) pro-inflammatory markers (iNOS, TNF-α, and IL-1β), (B) anti-inflammatory markers (Arg-1, IL-10, and CD206), and (C) inflammatory mediators (COX-2 and PGES2) mRNA levels by qRT-PCR. Data are expressed as mean ± SEM of four independent experiments. Statistical significance was determined by one-way ANOVA with a bonferroni post-test; $*P < 0.05$, $**P < 0.01$, $***P < 0.001$ compared to LPS-activated group. SEC: ADSC secretome.

2. ADSC secretome regulates NF-κB/AKT pathway with PTEN activation

For a mechanism study of controlling inflammation, NF-κB and AKT pathways are the first molecules to check. The pathways are closely related to induce inflammatory markers such as iNOS, TNF-α, and IL-6.[37,38] LPS induced the phosphorylation of NF-κB and AKT of RAW264.7 cells and ADSC secretome suppressed them in dose dependent (Fig. 3A-B). Also, 100 μg/ml of ADSC secretome induced PTEN expression significantly (Fig. 3A-C). To confirm the function of PTEN in effect of ADSC secretome, the PTEN inhibitor, SF1670 was applied with ADSC secretome. We checked the decrease of PTEN expression and increase of AKT phosphorylation by SF1670 (Fig. 4A-B). The effect of ADSC secretome to mRNA levels of pro-inflammatory and anti-inflammatory markers of macrophages were weakened by SF1670 (Fig. 4C-E). In short, ADSC secretome suppressed the phosphorylation of NF-κB and AKT with induction of PTEN expression of macrophage.

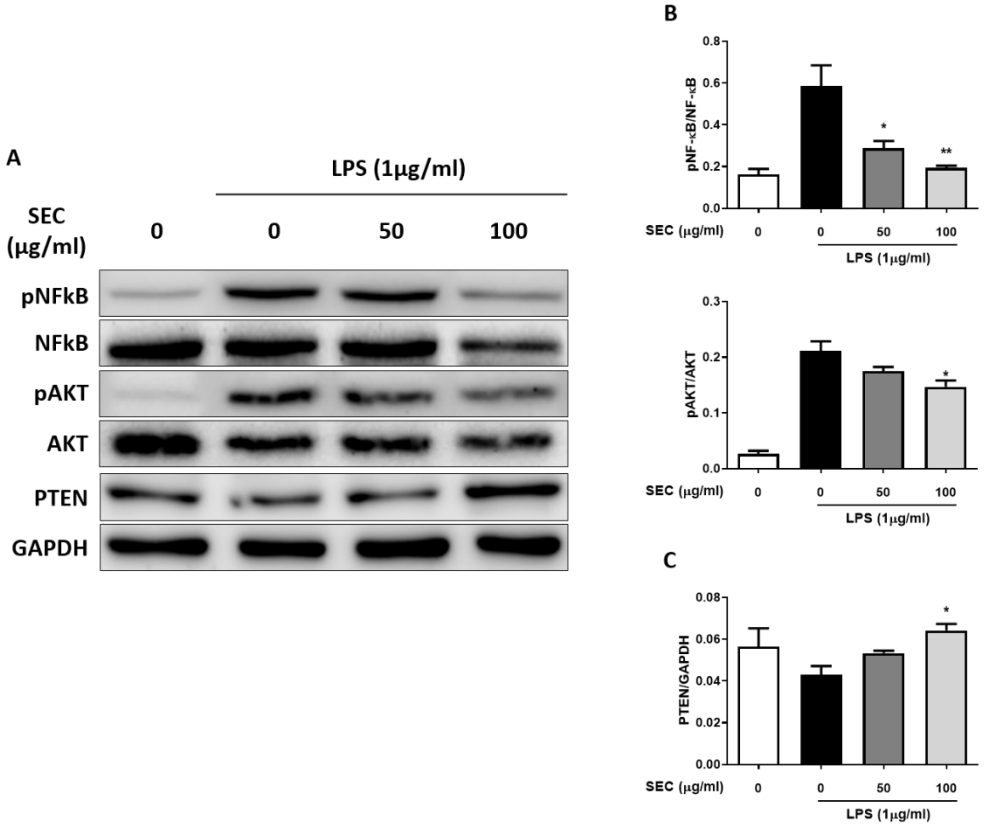

Figure 3. Regulation of NF-κB/AKT pathway of RAW264.7 cells by ADSC secretome in concentration dependent manner. RAW264.7 cells were activated with 1 μg/ml LPS and treated with 50 or 100 μg/ml ADSC secretome for 24 hr. (A) Immunoblots of NF-κB, AKT, and PTEN (B) Quantification of pNF-κB/NF-κB and pAKT/AKT levels; (C) PTEN/GAPDH level in RAW264.7 cells. Data are expressed as mean ± SEM of three independent experiments. Statistical significance was determined by one-way ANOVA with a bonferroni post-test; **P* < 0.05, ***P* < 0.01, compared to LPS-activated group. SEC: ADSC secretome.

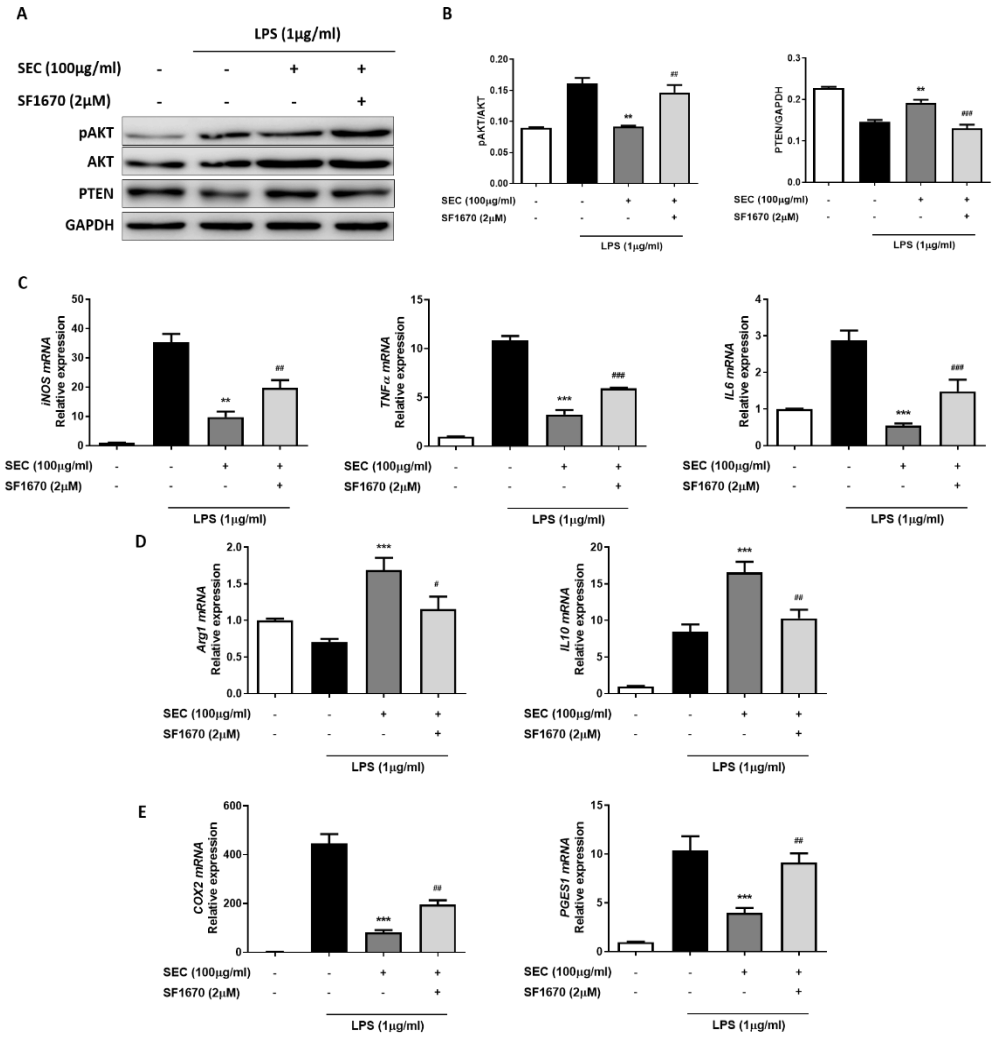

Figure 4. Restraint of the effect of ADSC secretome by PTEN inhibition. RAW264.7 cells were activated with 1 μg/ml LPS and treated with 100 μg/ml ADSC secretome in the absence or presence of 2 μM of SF1670 for 24 hr. (A) Immunoblots of AKT and PTEN. (B) Quantification of pAKT/AKT and PTEN/GAPDH levels in RAW264.7 cells. (C-E) Quantification of (C) pro-inflammatory markers (iNOS, TNF-α, and IL-1β), (D) anti-inflammatory markers (Arg-1, IL-10, and CD206), and (E) inflammatory mediators (COX-2 and PGES2) mRNA levels by qRT-PCR. Data are expressed as mean ± SEM of three

independent experiments. Statistical significance was determined by one-way ANOVA with a bonferroni post-test; $^{*}P < 0.05$, $^{**}P < 0.01$, $^{***}P < 0.001$ compared to LPS-activated group and $^{\#}P < 0.05$, $^{\#\#}P < 0.01$, $^{\#\#\#}P < 0.001$ compared to Secretome treatment group. SEC: ADSC secretome.

3. STAT/SOCS pathway is involved in the effect of ADSC secretome

As the other mechanism, which play crucial role in macrophage polarization, we observed STAT pathway with its regulator, SOCS proteins. Phosphorylation of STAT1, related to M1 polarization, was decreased and of STAT3, related to M2 polarization, was increased by ADSC secretome. An inhibitor of STAT1, SOCS1 and a mediator of negative feedback related to STAT3, SOCS3 were increased by ADSC secretome (Fig. 5A-B). With increase of SOCS1 and SOCS3 expressions, ADSC secretome regulated STAT1 and STAT3 phosphorylation to affect macrophage polarization.

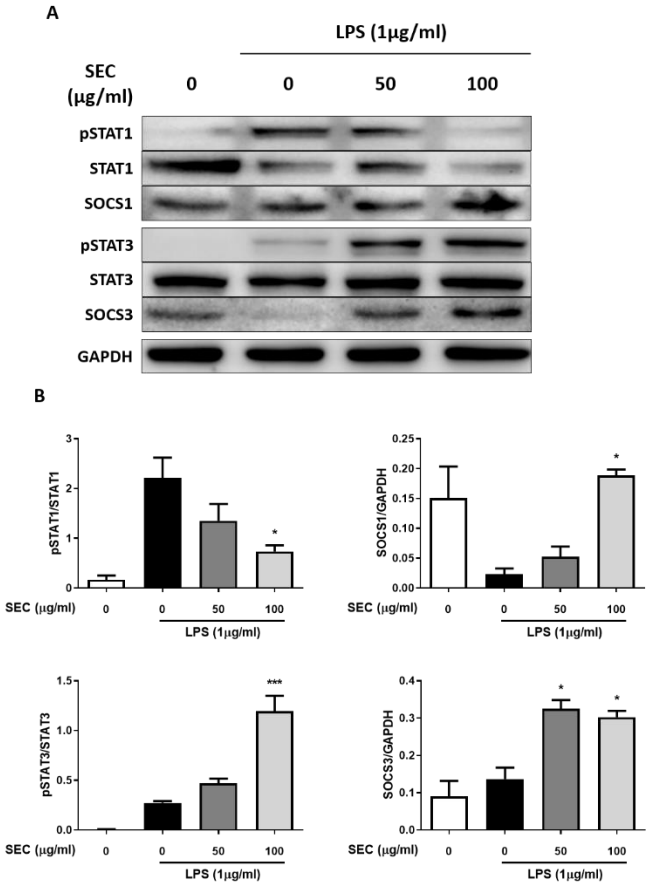

Figure 5. Regulation of STAT/SOCS pathway of RAW264.7 cells by ADSC secretome in concentration dependent manner. RAW264.7 cells were activated with 1 μg/ml LPS and treated with 50 or 100 μg/ml ADSC secretome for 24 hr. (A) Immunoblots of STAT1, SOCS1, STAT3, and SOCS3. (B) Quantification of pSTAT1/STAT1, SOCS1/GAPDH, pSTAT3/STAT3, and SOCS3/GAPDH levels in RAW264.7 cells. Data are expressed as mean ± SEM of three independent experiments. Statistical significance was determined by one-way ANOVA with a bonferroni post-test; *$P < 0.05$, ***$P < 0.001$ compared to LPS-activated group. SEC: ADSC secretome.

4. ADSC secretome improves the arthritis of CIA mice

To assess the therapeutic effect, ADSC secretome was treated to CIA mice 3 times a week for 4 weeks and as a control MTX was treated 2 times a week (Fig. 6A). ADSC secretome treated group (blue) lost bodyweight at 1 week of treatment, but gained bodyweight significantly at last compared to CIA untreated group (red) (Fig. 6B). Both ADSC secretome treated and MTX treated (yellow) groups showed lower arthritis score compared to CIA untreated group (Fig. 6C). ADSC secretome treated group, however, started to have lower arthritis score than CIA untreated group from 2.5 weeks of treatment and showed similar therapeutic result with MTX treated group at the end. (Fig. 6C). After 4 weeks of treatment, feet for all groups were observed and examined by histological analysis. CIA untreated group showed severe swollen paws and ankles but treatment groups showed mild swollen paws (Fig. 6D). Histological analysis of feet also showed improvement of cell infiltration, bone erosion, and synovial hyperplasia in treatment groups compared to CIA untreated group (Fig. 6E-F).

Peritoneal macrophages were isolated and analyzed with flow cytometry. Macrophages were gated by F4/80+ cells and a pro-inflammatory marker, CD86 and an anti-inflammatory marker, CD206 were observed. Secretome treated group showed decreased CD86 MFI and increased CD206 MFI significantly compared to CIA untreated group. MTX treated group, however, did not show any change compared to CIA untreated group (Fig 7). The results imply that ADSC secretome showed therapeutic effect to CIA with polarization of macrophages.

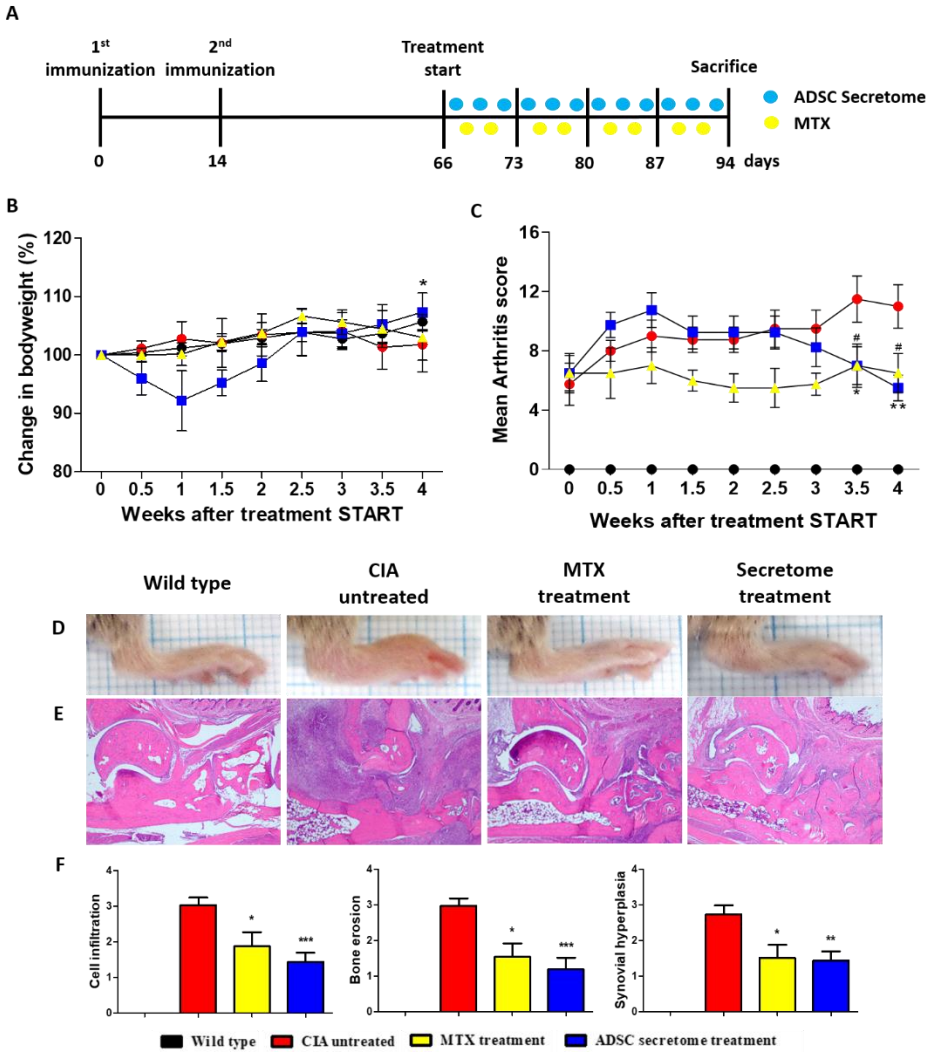

Figure 6. Therapeutic efficacy of ADSC secretome in CIA mice. (A) Schematic representation of MTX (35 mg/kg) and ADSC secretome (10 mg/kg) treatment to CIA mice. (B) Change in bodyweight based on weight at the first week of treatment and (C) Clinical arthritis score of CIA mice. (D) Representative photo showing feet of each group and (E) representative H&E images showing feet injury of each group. (F) Histological evaluation of H&E images with cell infiltration, bone erosion, and synovial hyperplasia. Data are

expressed as mean ± SEM (n = 4 per group). Statistical significance of figure B and C was determined by two-way ANOVA; *$P < 0.05$, **$P < 0.01$ for secretome treatment group and $^{\#}P < 0.05$ for MTX treatment group compared to CIA untreated group and of figure F was determined by one-way ANOVA with a bonferroni post-test; *$P < 0.05$, **$P < 0.01$, ***$P < 0.001$ compared to CIA untreated group. CIA: Collagen induced arthritis; MTX: Methotrexate.

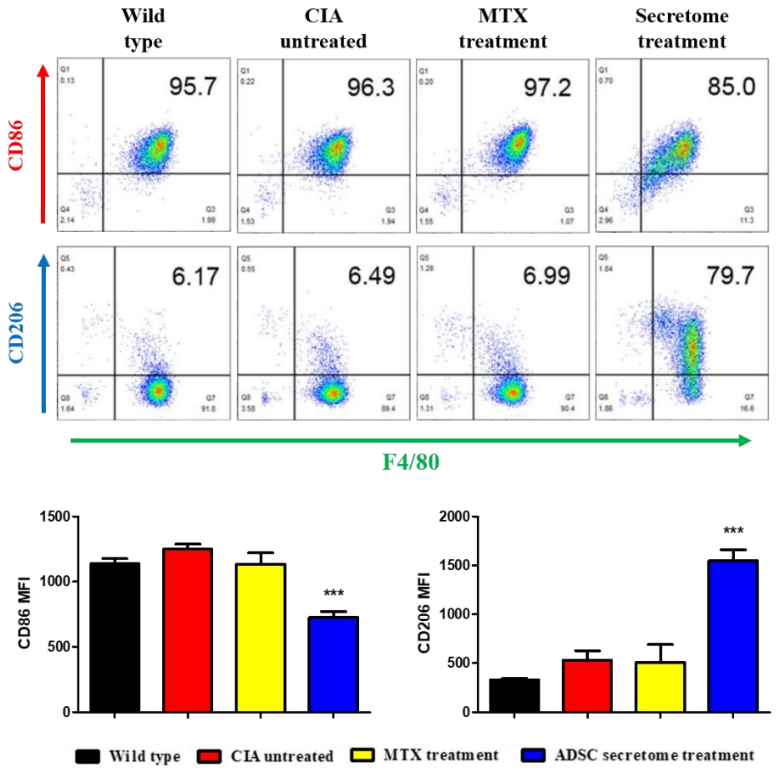

Figure 7. M2 polarization of peritoneal macrophage in CIA mice by ADSC secretome. Flow cytometry analysis of CD86 and CD206 in peritoneal macrophages of CIA. Data are expressed as mean ± SEM (n=4 per group). Statistical significance was determined by one-way ANOVA with a bonferroni post-test; ***$P < 0.001$ compared to CIA untreated group. CIA: Collagen induced arthritis; MTX: Methotrexate; MFI: Mean fluorescent intensity.

5. ADSC secretome shows therapeutic efficacy in NZB/W F1 mice

Experiment of treatment NZB/W F1 mice scheme was shown in Figure 8A. Bodyweight showed no change in treatment group (MPL: yellow and ADSC secretome: blue) compared to untreated group (red) except MPL treatment group showing higher bodyweight on 27 weeks old (Fig. 8B). Proteinuria of the untreated group was increased continuously and of treatment group showed significant difference compared to untreated group starting from 26 weeks old (Fig. 8C). Histological analysis of kidney showed improved renal damage as having lower histopathological score in ADSC secretome treatment group similar to MPL treatment group (Fig. 8D-E).

Isolated peritoneal macrophages of ADSC secretome treatment group showed high CD206 MFI, but no change in CD86 MFI and of MPL treatment group did not show any change in both markers (Fig. 9).

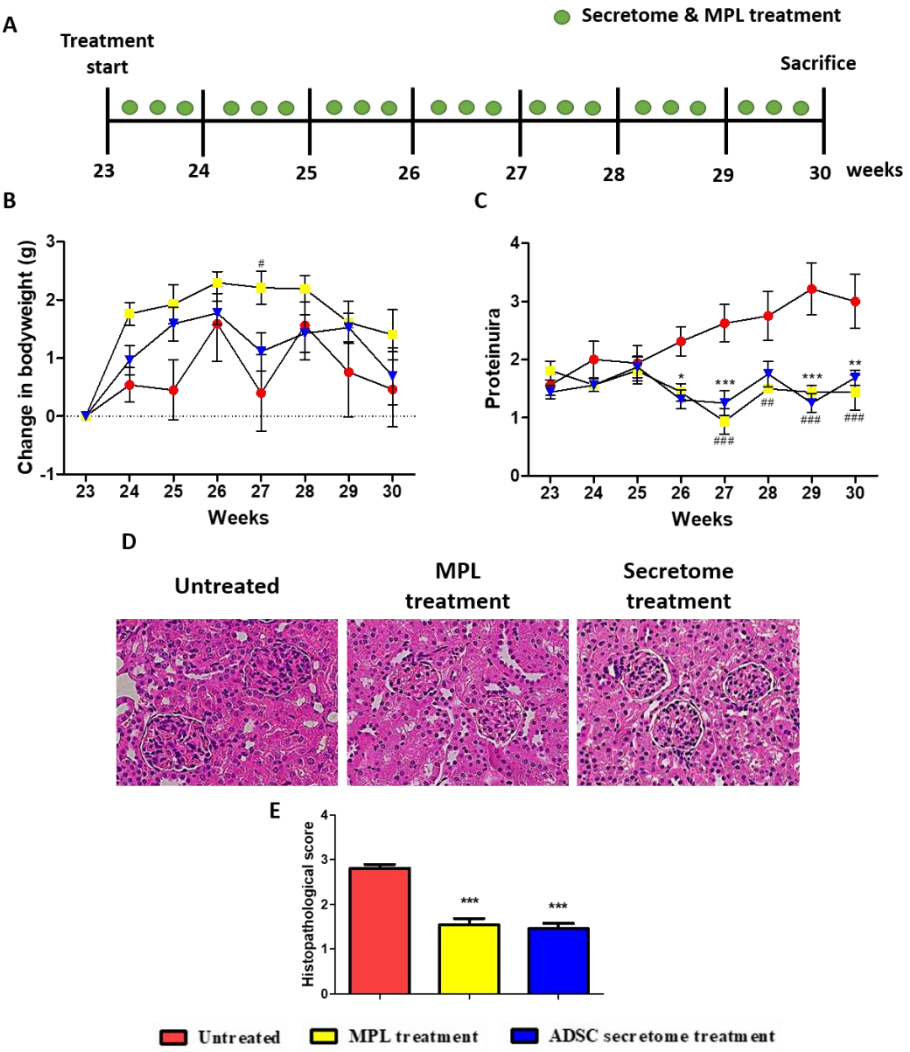

Figure 8. Therapeutic efficacy of ADSC secretome in NZB/W F1 mice. (A) Schematic representation of MPL (7 mg/kg) and ADSC secretome (10 mg/kg) treatment to NZB/W F1 mice. (B) Change in bodyweight based on weight at 23 weeks old and (C) proteinuria of NZB/W F1 mice. (D) Representative H&E images showing kidney injury and (F) histological evaluation. Data are expressed as mean ± SEM (n = 8 per group). Statistical significance of figure B and C was determined by two-way ANOVA; *$P < 0.05$, **$P < 0.01$,

***$P < 0.001$ for secretome treatment group and $^{\#}P < 0.05$, $^{\#\#}P < 0.01$, $^{\#\#\#}P < 0.001$ for MPL treatment group compared to untreated group and of figure E was determined by one-way ANOVA with a bonferroni post-test; ***$P < 0.001$ compared to untreated group. MPL: Methylprednisolone.

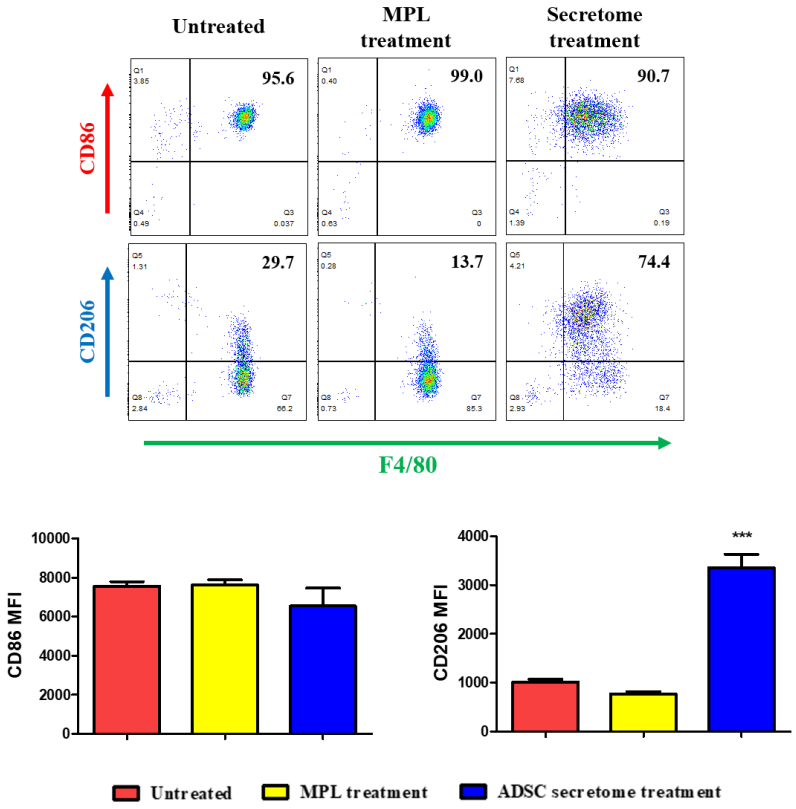

Figure 9. M2 polarization of peritoneal macrophage in NZB/W F1 mice by ADSC secretome. Flow cytometry analysis of CD86 and CD206 in F4/80^{+} macrophages of NZB/W F1. Data are expressed as mean ± SEM (n = 8 per group). Statistical significance was determined by one-way ANOVA with a bonferroni post-test; ***$P < 0.001$ compared to untreated group. MPL: Methylprednisolone; MFI: Mean fluorescent intensity.

6. Peritoneal macrophages in the steady state are switched to M2 phenotype by ADSC secretome

Unlike RAW264.7 cells, viability of peritoneal macrophages was increased in dose dependent (Fig. 10A). Sun et al. reported that M2 subtype of macrophages induced by adipose MSCs or IL-4/-13 have high cell viability with strong adherence ability.[29] As observed in vitro assay, ADSC secretome decreased CD86 MFI and increased CD206 MFI in dose dependent. Especially, CD86 MFI was decreased to a large extent (Fig. 10B). Other representative markers of macrophage, iNOS and Arg-1 were examined by qRT-PCR and western blot. iNOS was suppressed and Arg-1 was induced by ADSC secretome in dose dependent (Fig. 10C-E). Like CD86, expression of Arg-1 was highly increased in both mRNA and protein levels. The mRNA levels of pro- and anti-inflammatory markers of macrophage were analyzed further. CD86, TNF-α, IL-6, IL-12p40, and IL-1β were decreased (Fig. 11A) and CD206, TGF-β1, and IL-10 were increased by ADSC secretome in dose dependent (Fig. 11B). Taken together, ADSC secretome decreased M1 markers and increased M2 markers of peritoneal macrophages in the steady state.

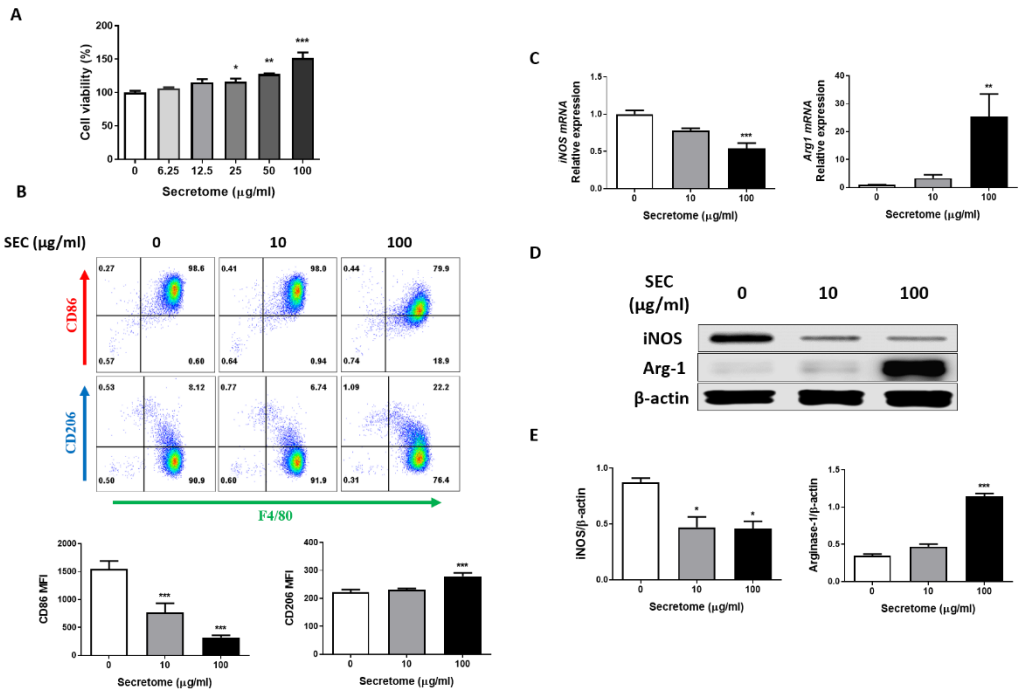

Figure 10. M2 polarization of peritoneal macrophage by ADSC secretome. (A) Cell viability of peritoneal macrophages incubated for 24 hr with the ADSC secretome at various concentrations. (B-I) Peritoneal macrophages were treated with with 10 or 100 μg/ml ADSC secretome for 24 hr. (B) Flow cytometry analysis of CD86 and CD206 in F4/80^{+} macrophages. (C) Quantification of iNOS and Arg-1 mRNA levels by qRT-PCR. (D) Immunoblots of iNOS and Arg-1. (E) Quantification of iNOS/β-actin and Arg-1/β-actin in peritoneal macrophages. Data are expressed as mean ± SEM of four independent experiments. Statistical significance was determined by one-way ANOVA with a bonferroni post-test; *$P < 0.05$, **$P < 0.01$, ***$P < 0.001$ compared to control group. MFI: Mean fluorescent intensity.

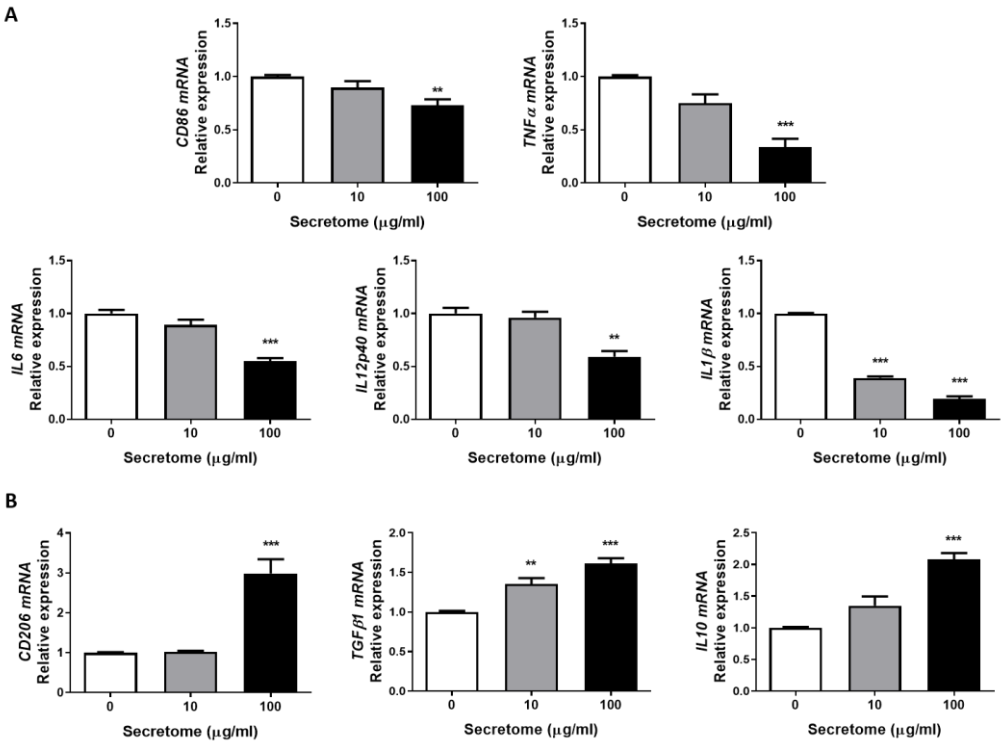

Figure 11. Change gene expression of peritoneal macrophage to M2 phenotype by ADSC secretome. Peritoneal macrophages were treated with 10 or 100 μg/ml ADSC secretome for 24 hr. Quantification of (A) pro-inflammatory markers (CD86, TNF-α, IL-6, IL-12p40, and IL-1β) and (B) anti-inflammatory markers (CD206, TGF-β1, and IL-10) mRNA levels by qRT-PCR. Data are expressed as mean ± SEM of four independent experiments. Statistical significance was determined by one-way ANOVA with a bonferroni post-test; $^{**}P < 0.01$, $^{***}P < 0.001$ compared to the control group.

7. ADSC secretome also regulate inflammatory activity of LPS-stimulated peritoneal macrophages

We also tested the effect of ADSC secretome to LPS-stimulated peritoneal macrophages. CD86 MFI (Fig. 12A) and mRNA level of iNOS (Fig. 12B) were suppressed by ADSC secretome. ADSC secretome did not change CD206 MFI (Fig. 12A) but increase mRNA level of Arg-1 (Fig. 12B). Similar to the result of steady state, mRNA expressions of pro-inflammatory markers, CD86, TNF-α, IL-6, and IL-1β of LPS stimulated peritoneal macrophages were decreased significantly by ADSC secretome (Fig. 13A). ADSC secretome induced IL-10 mRNA expression of LPS stimulated peritoneal macrophages apparently. CD206 mRNA expression of LPS stimulated peritoneal macrophages was also increased significantly by ADSC secretome; however, it showed a slight increase similar to the flow cytometry result (Fig. 13B). ADSC secretome also restrained phosphorylation of NF-κB and AKT of LPS stimulated peritoneal macrophages significantly (Fig. 14A-B). These results suggest that activated peritoneal macrophages are also regulated by ADSC secretome.

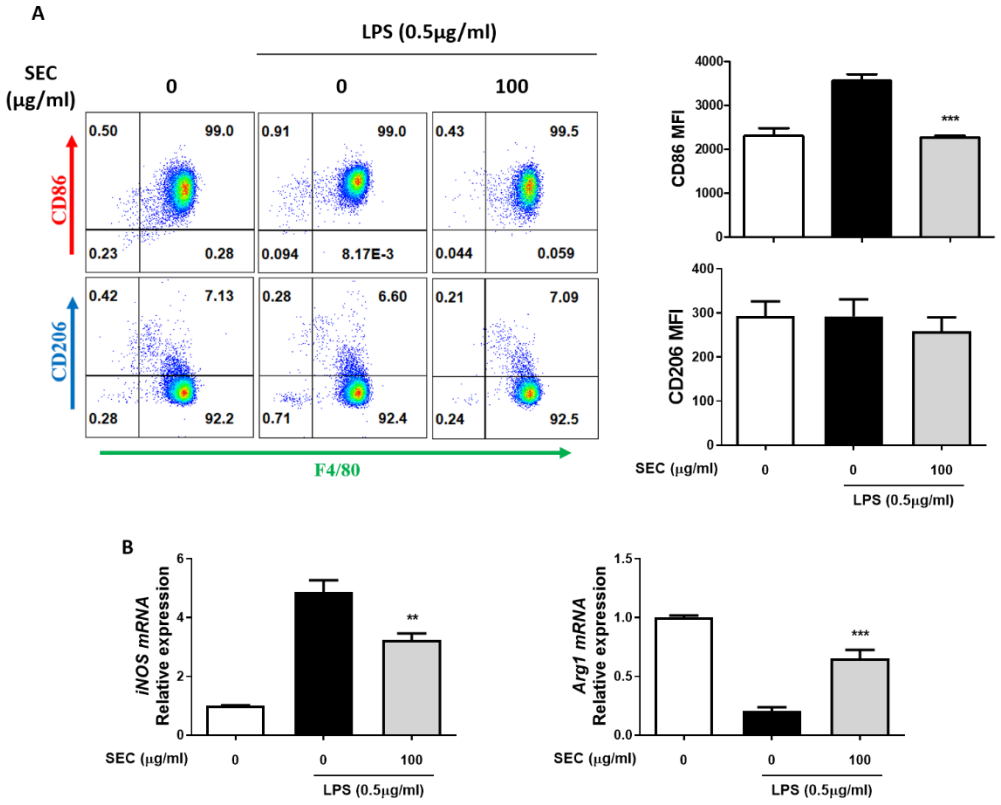

Figure 12. M2 polarization of LPS-stimulated peritoneal macrophage by ADSC secretome. Peritoneal macrophages were treated with 100 μg/ml ADSC secretome for 24 hr and stimulated with 0.5 μg/ml LPS for 3 hr. (A) Flow cytometry analysis of CD86 and CD206 in $F4/80^{+}$ macrophages (B) Quantification of iNOS and Arg-1 mRNA levels by qRT-PCR. Data are expressed as mean ± SEM of four independent experiments. Statistical significance was determined by one-way ANOVA with a bonferroni post-test; $^{**}P < 0.01$, $^{***}P < 0.001$ compared to LPS stimulated group. SEC: ADSC secretome; MFI: Mean fluorescent intensity.

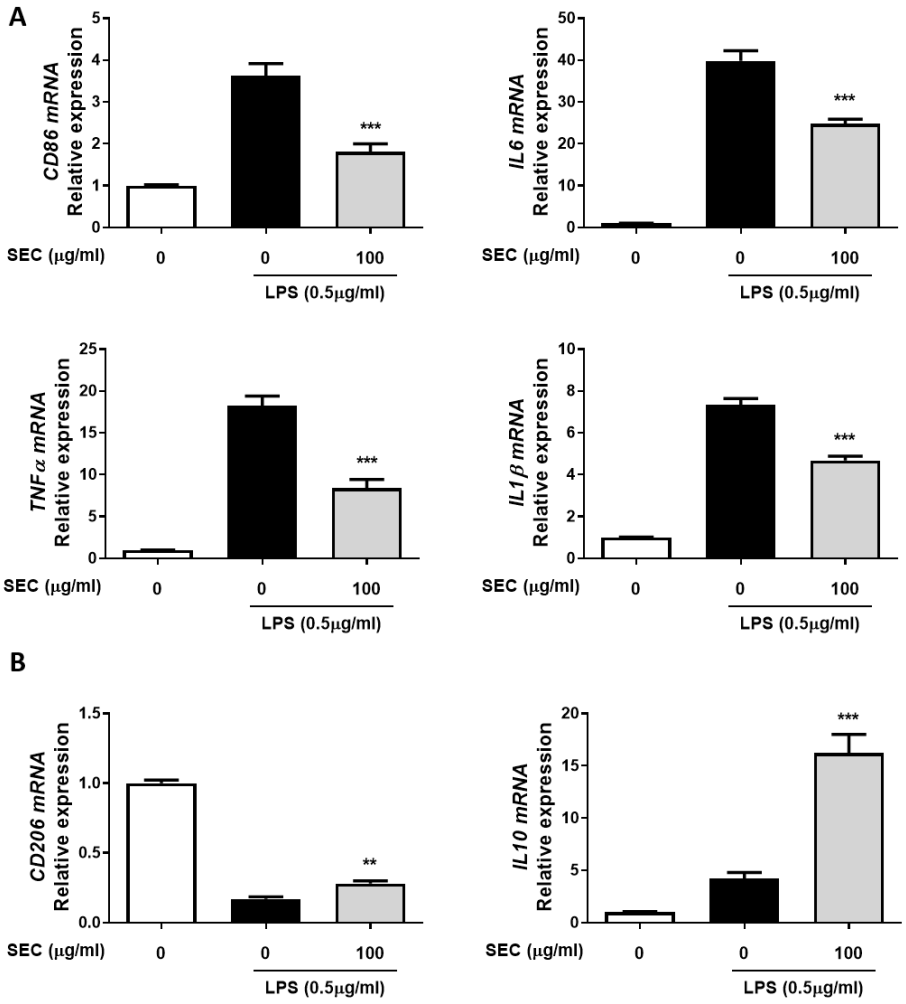

Figure 13. Change gene expression of LPS-stimulated peritoneal macrophage to M2 phenotype by ADSC secretome. Peritoneal macrophages were treated with 100 μg/ml ADSC secretome for 24 hr and stimulated with 0.5 μg/ml LPS for 3 hr. Quantification of (A) pro-inflammatory markers (CD86, TNF-α, IL-6, and IL-1β) and (B) anti-inflammatory markers (CD206 and IL-10) mRNA levels by qRT-PCR. Data are expressed as mean ± SEM of four independent experiments. Statistical significance was determined by one-way

ANOVA with a bonferroni post-test; $^{**}P < 0.01$, $^{***}P < 0.001$ compared to the LPS stimulated group. SEC: ADSC secretome.

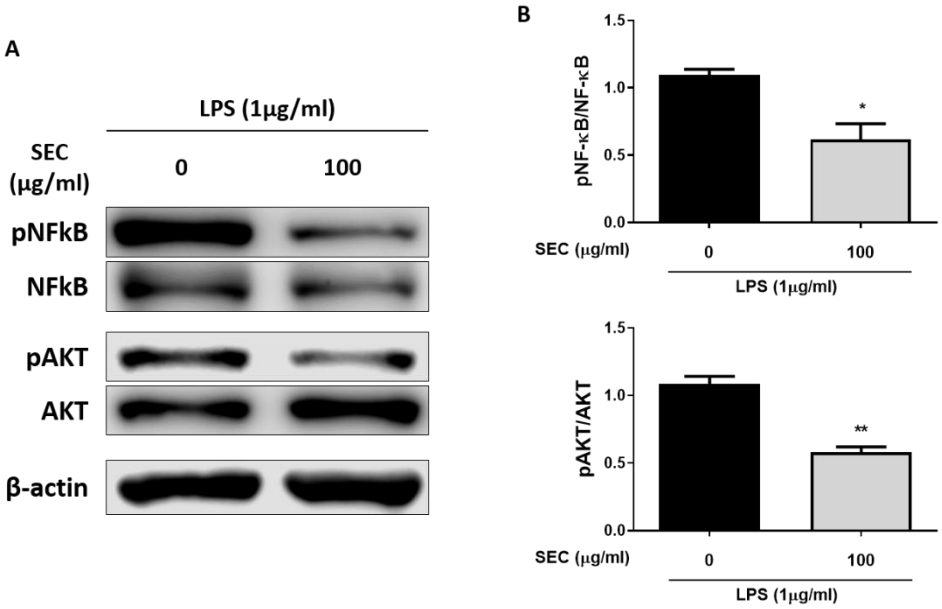

Figure 14. Reduction of NF-κB/AKT phosphorylation of LPS-stimulated peritoneal macrophage by ADSC secretome. Peritoneal macrophages were treated with 100 μg/ml ADSC secretome for 24 hr and stimulated with 1 μg/ml LPS for 3 hr. (A) Immunoblots of NF-κB and AKT. (B) Quantification of pNF-κB/NF-κB and pAKT/AKT levels. Data are expressed as mean ± SEM of three independent experiments. Statistical significance was determined by one-way ANOVA with a bonferroni post-test; $^{*}P < 0.05$, $^{**}P < 0.01$, compared to the LPS stimulated group. SEC: ADSC secretome.

8. ADSC secretome controls the secretion of cytokines of peritoneal macrophages

Released cytokine levels of peritoneal macrophages were examined with cultured supernatants by ELISA. TNF-α and IL-1β levels were decreased (Fig. 15A) and IL-10 level was increased (Fig. 15C) by ADSC secretome significantly in both environments. Especially, secretion of IL-6 was elevated in the steady state, whereas it was reduced in the LPS stimulated state by ADSC secretome (Fig. 15B).

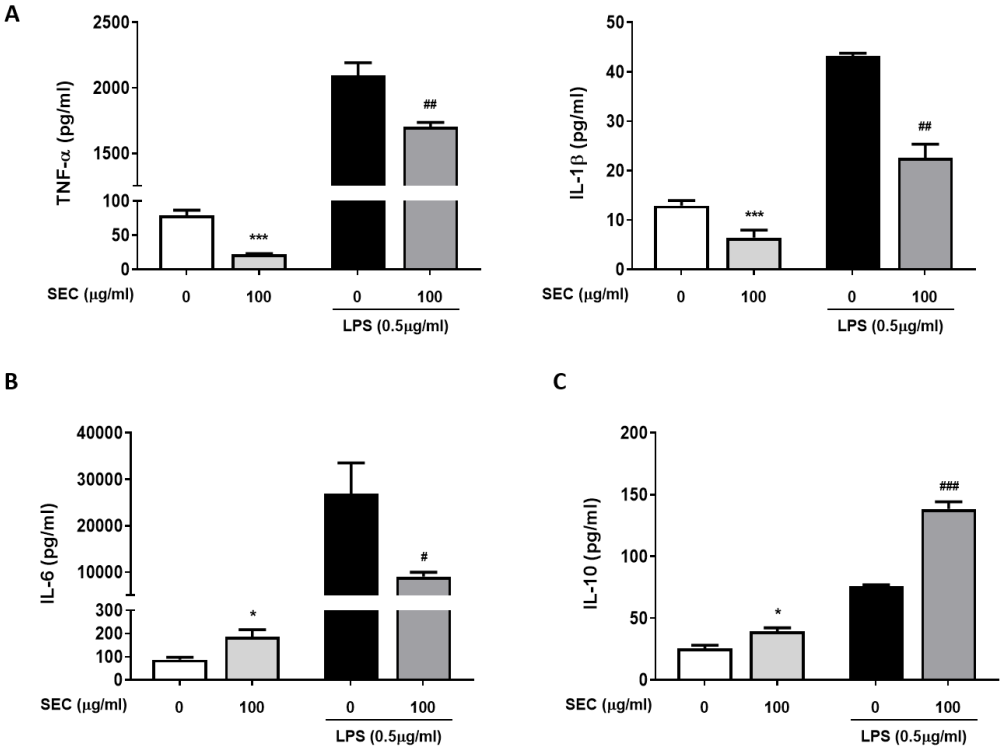

Figure 15. Regulation of cytokine secretion of peritoneal macrophage by ADSC secretome. Quantification of (A) TNF-α, IL-1β, (B) IL-6 and (C) IL-10 in culture supernatant by ELISA. Data are expressed as mean ± SEM of four independent experiments. Statistical significance was determined by one-way ANOVA with a bonferroni post-test; $*P < 0.05$, $***P < 0.001$ compared to control group and $^{\#}P < 0.05$, $^{\#\#}P < 0.01$, $^{\#\#\#}P < 0.001$ compared LPS-stimulated group. SEC: ADSC secretome.

9. ADSC secretome induces M2b/c-like phenotype of peritoneal macrophages

To analyze macrophages polarization in more details, M2 subtypes were observed with Ym-1 (M2a), SPHK1 (M2b), LIGHT (M2b), and MerTK (M2c) as markers. In the steady state, only MerTK and LIGHT mRNA levels were increased by ADSC secretome. LPS-stimulated macrophages, however, showed increased all M2 subtype markers by ADSC secretome (Fig. 16A). In addition to qRT-PCR result, membranous LIGHT and MerTK were examined by flow cytometry. Similar to mRNA levels, LIGHT and MerTK MFI were increased by ADSC secretome (Fig. 16B). Taken together, ADSC secretome affects M2 polarization toward M2b/c as LIGHT and MerTK increases mainly.

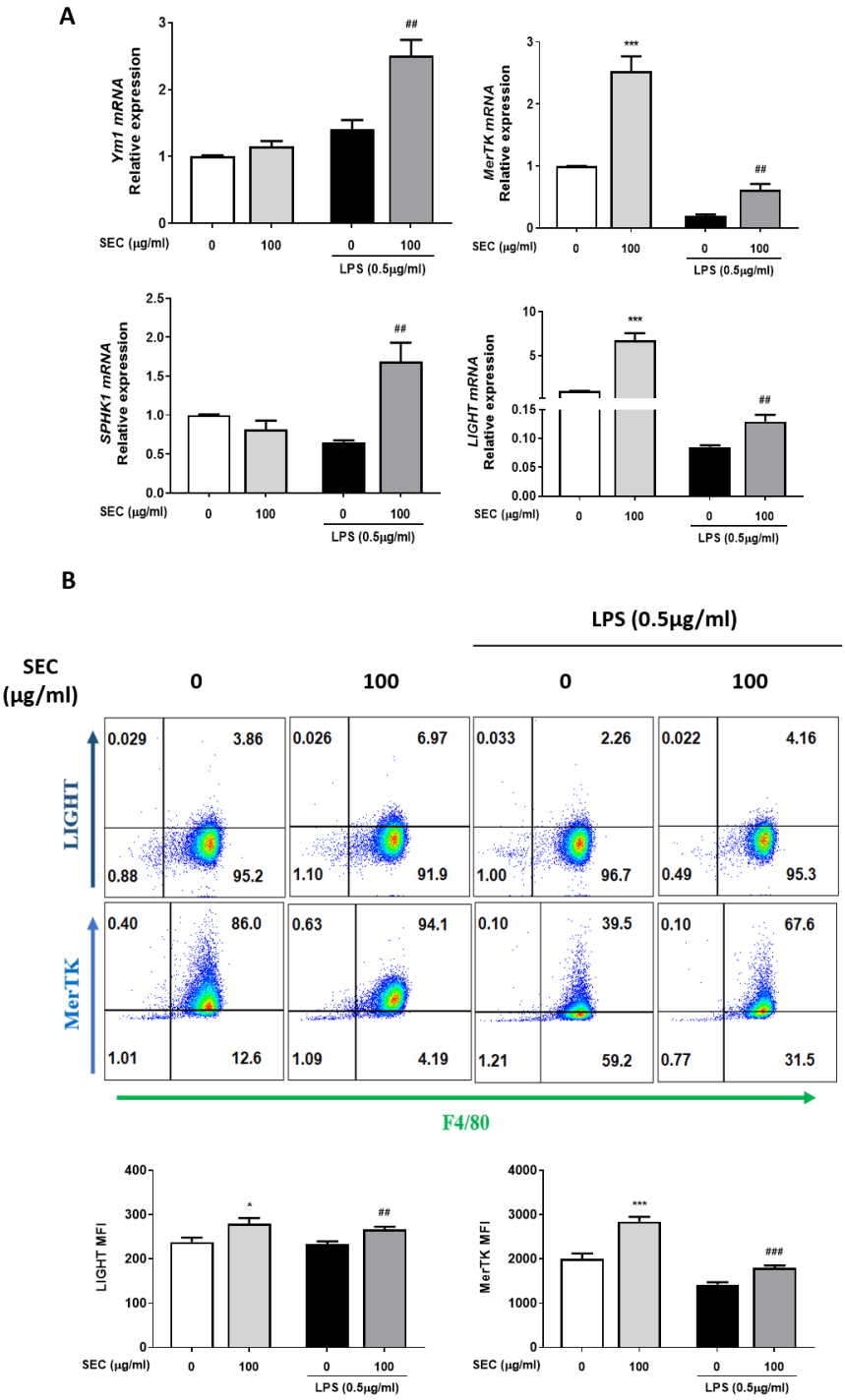

Figure 16. Involvement of ADSC secretome to M2 subtype polarization of peritoneal macrophages. Peritoneal macrophages treated with 100 μg/ml ADSC secretome for 24 hr in the absence or presence of 0.5 μg/ml LPS stimulation. (A) Quantification of Ym-1, SPHK1, LIGHT, and MerTK mRNA levels by qRT-PCR. (B) Flow cytometry analysis of LIGHT and MerTK in $F4/80^{+}$ macrophages. Data are expressed as mean ± SEM of four independent experiments. Statistical significance was determined by one-way ANOVA with a bonferroni post-test; $^{*}P < 0.05$, $^{***}P < 0.001$ compared to control group and $^{\#\#}P < 0.01$, $^{\#\#\#}P < 0.001$ compared LPS-stimulated group. SEC: ADSC secretome; MFI: Mean fluorescent intensity.

10. Compositions of ADSC secretome are analyzed

First, patterns of secreted proteins from 3 sets of ADSC secretome (SEC #1, #2, and #3) were examined with the result of 1D SDS-PAGE. Even though strong similar patterns at ~70kDa were observed between SEC #1 and SEC #2, total protein patterns were similar between SEC #1 and SEC #3 (Fig. 17A). For further analysis, 2D SDS-PAGE was performed and similar patterns between SEC #1 and SEC #3 were confirmed. There was a specific pattern (blue arrow) that only show at SEC #1 and SEC #3 at ~150 kDa and one spot at ~42 kDa (green arrow) has similar density at SEC #1 and SEC #3 but not at SEC #2 (Fig. 17B).

Then, the 2D-PAGE result of SEC #1 was subjected to LC/MS-MS analysis and 84 proteins were identified (Table. 1). Functional enrichment analysis of the proteins was carried out using DAVID software. Each 10 gene ontology terms (p value ≤ 0.05) of biological processes (BP), molecular function (MF), and cell component (CC) was listed in order of highest count with p value. Representative gene ontology terms of BP (Fig. 18A) include cell adhesion, intermediate filament organization, and extracellular matrix organization (-Log10(p value) = 4.03, 9.44, and 6.03, respectively). Major gene ontology terms of MF (Fig. 18B) include protein binding, calcium ion binding, and identical protein binding (-Log10(p value) = 1.89, 6.30, and 2.34, respectively). Gene ontology terms of CC (Fig. 18C) include extracellular exosome, extracellular spaced, and extracellular region (-Log10(p value) = 34.9, 31.6, and 26.3, respectively).

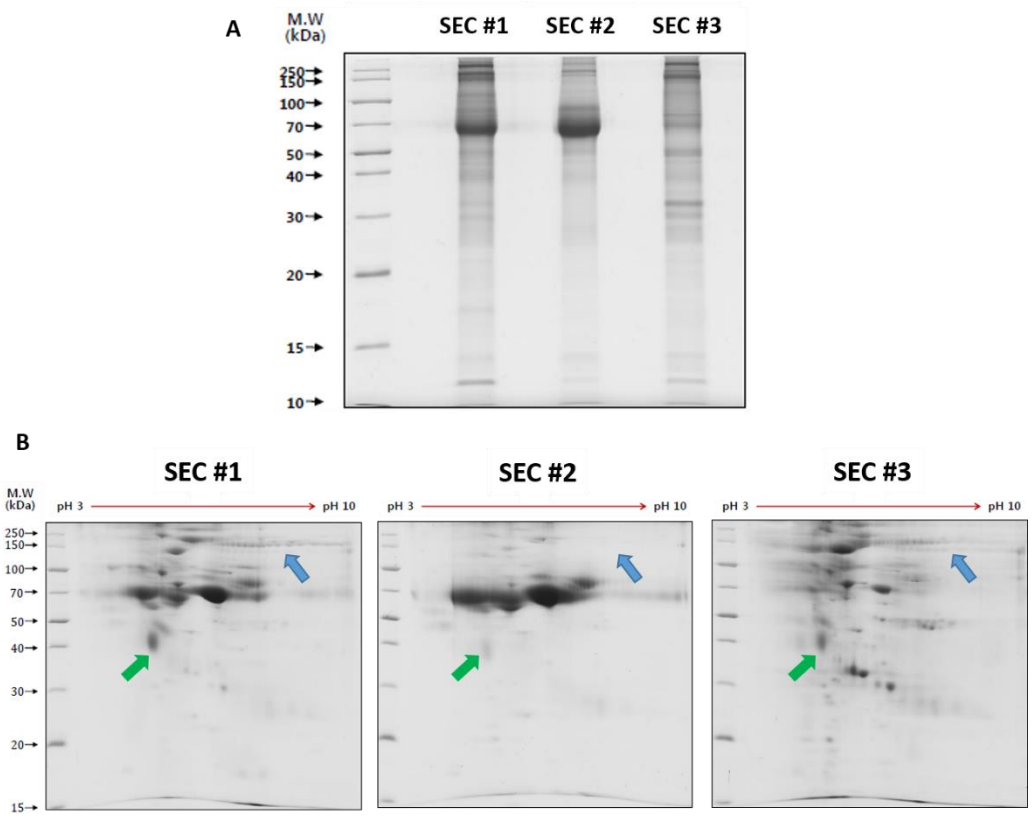

Figure 17. Protein component analysis of ADSC secretome with 1D and 2D SDS-PAGE. Images of (A) 1D and (B) 2D SDS PAGE with three sets (SEC #1, SEC #2, and SEC #3) of ADSC secretome from three different donors. SEC: ADSC secretome

Table 2. 84 proteins by LC/MS-MS proteomics analysis

Uniprot_ID	Accession	Gene	Protein
MMP2_HUMAN	P08253	MMP2	72 kDa type IV collagenase
ACTB_HUMAN	P60709	ACTB	Actin, cytoplasmic 1
ACTN1_HUMAN	P12814	ACTN1	Actinin alpha 1
ACTN4_HUMAN	O43707	ACTN4	Actinin alpha 4
Q562M3_HUMAN	Q562M3	ACT	Actin-like protein
FETUA_HUMAN	P02765	AHSG	Alpha-2-HS-glycoprotein
A2MG_HUMAN	P01023	A2M	alpha-2-macroglobulin
L8E9Z3_HUMAN	L8E9Z3	HRC	Alternative protein HRC
ANXA1_HUMAN	P04083	ANXA1	Annexin A1
B4GA1_HUMAN	O43505	B4GAT1	Beta-1,4-glucuronyltransferase 1
BTD_HUMAN	P43251	BTD	Biotinidase
CO1A1_HUMAN	P02452	COL1A1	Collagen alpha-1(I) chain
CO3A1_HUMAN	P02461	COL3A1	Collagen alpha-1(III) chain
CO6A1_HUMAN	P12109	COL6A1	Collagen alpha-1(VI) chain
CO1A2_HUMAN	P08123	COL1A2	Collagen alpha-2(I) chain
CO5A2_HUMAN	P05997	COL5A2	Collagen alpha-2(V) chain
CO6A3_HUMAN	P12111	COL6A3	Collagen alpha-3(VI) chain
CFAH_HUMAN	P08603	CFH	Complement factor H
C1R_HUMAN	P00736	C1r	Complement C1r subcomponent
C1S_HUMAN	P09871	C1s	Complement C1s subcomponent
CFAB_HUMAN	P00751	CFB	Complement factor B
F5BAB3_HUMAN	F5BAB3	CYTB	Cytochrome b
PGS2_HUMAN	P07585	DCN	Decorin
DCD_HUMAN	P81605	DCD	Dermcidin
DSG1_HUMAN	Q02413	DSG1	Desmoglein-1
DKK3_HUMAN	Q9UBP4	DKK3	dickkopf WNT signaling pathway inhibitor 3
EF2_HUMAN	P13639	EEF2	Elongation factor 2
EMIL2_HUMAN	Q9BXX0	EMILIN2	EMILIN-2
CD248_HUMAN	Q9HCU0	CD248	Endosialin

FBN1_HUMAN	P35555	FBN1	Fibrillin-1
FINC_HUMAN	P02751	FN1	Fibronectin
FBLN1_HUMAN	P23142	FBLN1	Fibulin-1
FSTL1_HUMAN	Q12841	FSTL1	Follistatin-related protein 1
LG3BP_HUMAN	Q08380	LGALS3BP	Galectin-3-binding protein
GELS_HUMAN	P06396	GSN	Gelsolin
HSP13_HUMAN	P48723	HSPA13	Heat shock 70 kDa protein 13
ISLR_HUMAN	O14498	ISLR	Immunoglobulin superfamily containing leucine-rich repeat protein
IBP6_HUMAN	P24592	IGFBP6	Insulin-like growth factor-binding protein 6
ITIH2_HUMAN	P19823	ITIH2	Inter-alpha-trypsin inhibitor heavy chain H2
K1C10_HUMAN	P13645	KRT10	Keratin, type I cytoskeletal 10
K1C14_HUMAN	P02533	KRT14	Keratin, type I cytoskeletal 14
K1C16_HUMAN	P08779	KRT16	Keratin, type I cytoskeletal 16
K1C9_HUMAN	P35527	KRT9	Keratin, type I cytoskeletal 9
K2C1_HUMAN	P04264	KRT1	Keratin, type II cytoskeletal 1
K22E_HUMAN	P35908	KRT2	Keratin, type II cytoskeletal 2 epidermal
K2C5_HUMAN	P13647	KRT5	Keratin, type II cytoskeletal 5
K2C6B_HUMAN	P04259	KRT6B	Keratin, type II cytoskeletal 6B
K2C6C_HUMAN	P02538	KRT6C	Keratin, type II cytoskeletal 6C
TRFL_HUMAN	P02788	LTF	Lactotransferrin
LAMB1_HUMAN	P07942	LAMB1	Laminin subunit beta-1
LAMC1_HUMAN	P11047	LAMC1	Laminin subunit gamma-1
LUM_HUMAN	P51884	LUM	Lumican
MOES_HUMAN	P26038	MSN	Moesin
NID1_HUMAN	P14543	NID1	Nidogen-1
NUCB1_HUMAN	Q02818	NUCB1	Nucleobindin-1
OLFL3_HUMAN	Q9NRN5	OLFML3	Olfactomedin-like protein 3
PTX3_HUMAN	P26022	PTX3	Pentraxin-related protein PTX3
PEDF_HUMAN	P36955	SERPINF1	Pigment epithelium-derived factor
IC1_HUMAN	P05155	SERPING1	Plasma protease C1 inhibitor
PLOD1_HUMAN	Q02809	PLOD1	Procollagen-lysine,2-oxoglutarate 5-dioxygenase 1

PE2R4_HUMAN	P35408	PTGER4	Prostaglandin E2 receptor EP4 subtype
PDIA3_HUMAN	P30101	PDIA3	Protein disulfide-isomerase A3
PTMA_HUMAN	P06454	PTMA	Prothymosin alpha
KPYM_HUMAN	P14618	PKM	Pyruvate kinase PKM
GDIA_HUMAN	P31150	GDI1	Rab GDP dissociation inhibitor alpha
RLGPB_HUMAN	Q86X10	RALGAPB	Ral GTPase-activating protein subunit beta
ARH37_HUMAN	A1IGU5	ARHGEF37	Rho quanine nucleotide exchange factor 37
PRPC_HUMAN	P02810	PRH1	Salivary acidic proline-rich phosphoprotein 1/2
ANT3_HUMAN	P01008	SERPINC1	Serpin family C member 1
S12A7_HUMAN	Q9Y666	SLC12A7	Solute carrier family 12 member 7
SPRC_HUMAN	P09486	SPARC	SPARC
TRAC_HUMAN	P01848	TRAC	T cell receptor alpha chain constant
TIAM2_HUMAN	Q8IVF5	TIAM2	T-lymphoma invasion and metastasis-inducing protein 2
BGH3_HUMAN	Q15582	TGFBI	Transforming growth factor beta induced
TKT_HUMAN	P29401	TKT	Transketolase
Q3T7B8_HUMAN	Q3T7B8	TRIT1	tRNA isopentenylpyrophosphate transferase isoform 5
ADAT1_HUMAN	Q9BUB4	ADAT1	tRNA-specific adenosine deaminase 1
SYWC_HUMAN	P23381	WARS1	Tryptophan--tRNA ligase, cytoplasmic
VASN_HUMAN	Q6EMK4	VASN	Vasorin
VIME_HUMAN	P08670	VIM	Vimentin
VTDB_HUMAN	P02774	GC	Vitamin D-binding protein
PROS_HUMAN	P07225	PROS1	Vitamin K-dependent protein S
VTNC_HUMAN	P04004	VTN	Vitronectin
WDR1_HUMAN	O75083	WDR1	WD repeat-containing protein 1

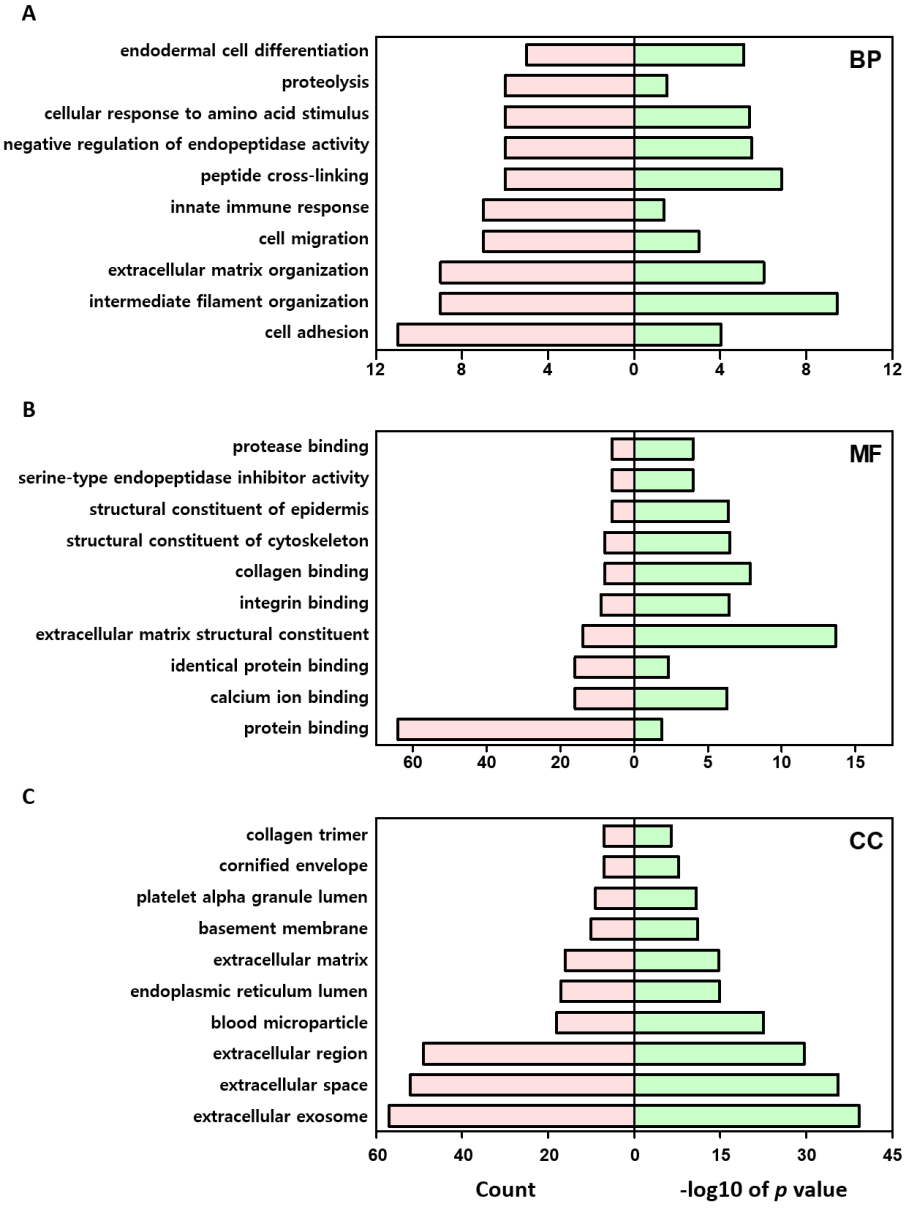

Figure 18. Functional enrichment analysis of ADSC secretome. Count and *p* value of major GO terms of biological processes (BP; A), molecular functions (MF; B), and cellular components (CC; C).

11. Candidate molecules of the effect toward macrophage are identified

First, proteins which contain secreted, immune response, and inflammation as keywords of DAVID bioinformatics analysis were selected among 84 proteins. As patterns of electrophoresis were similar between SEC #1 and SEC #3, we compared the effect of three ADSC secretome sets toward peritoneal macrophage. CD86 MFI of peritoneal macrophages was decreased to a similar extent by SEC #1 and SEC #3; however, it was decreased slightly by SEC #2 (Fig. 18A). Based on the result of patterns and CD86 MFI, 36 common spots that have fold change < 2 between SEC #1 and SEC #3 were selected through image analysis (Fig. 18B and Table. 3). Finally, 7 candidate molecules were listed and pentraxin-3 (PTX3) and Galectin 3 binding protein (LGALS3BP) were selected for further analysis (Table. 3)

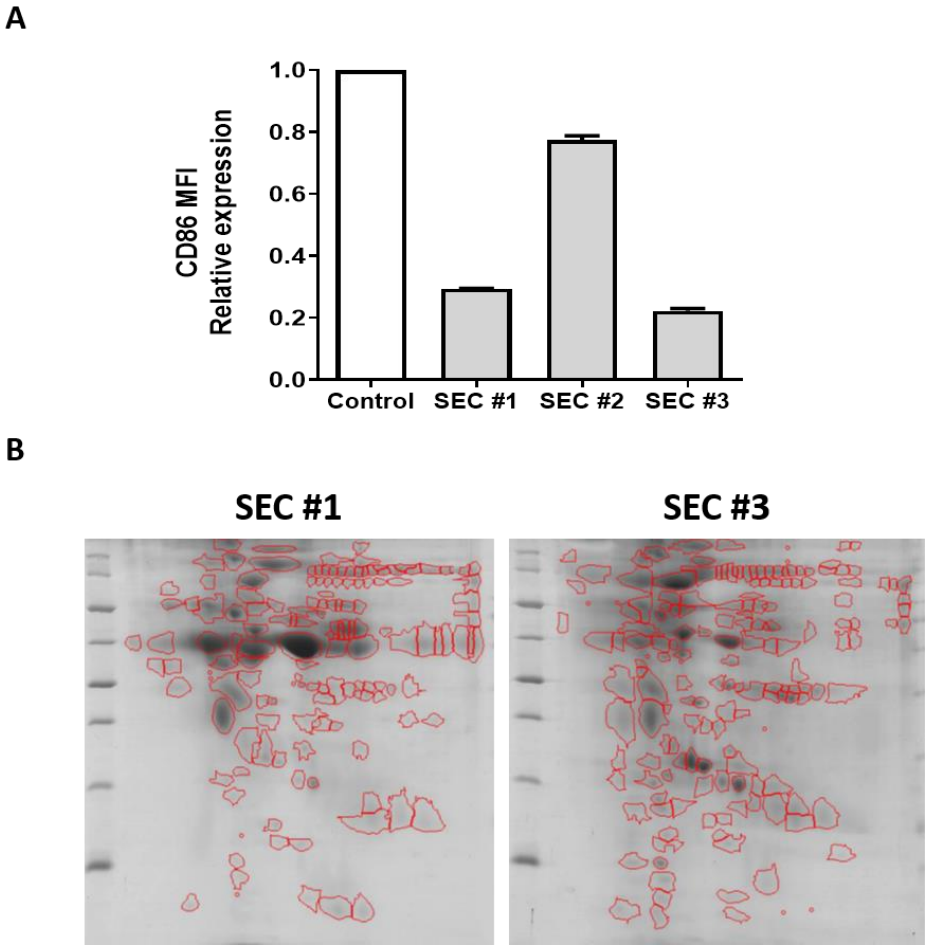

Figure 19. Strategy of exploring candidate molecules of the effect from ADSC secretome. (A) Relative expression of CD86 MFI of peritoneal macrophages treated with three sets of secretome. (B) Image analysis of 2D SDS-PAGE of SEC #1 and SEC #3 to select spots. Data are expressed as mean ± SEM of three independent experiments.

Table 3. Spots having similar intensity between SEC #1 and SEC #3

Spot	SEC #1	SEC #3	Ratio
1	2.748	2.518	1.091
2	2.312	1.992	1.161
3	1.365	1.011	1.350
4	0.809	0.865	1.069
5	0.436	0.415	1.049
6	0.472	0.472	1.002
7	0.340	0.217	1.569
8	0.592	0.606	1.024
9	0.621	0.647	1.041
10	0.768	0.652	1.178
11	0.544	0.3	1.815
12	0.596	0.303	1.968
13	0.455	0.462	1.017
14	7.931	13.376	1.687
15	0.149	0.226	1.511
16	0.188	0.238	1.269
17	0.181	0.259	1.434
18	0.179	0.207	1.160
19	0.158	0.176	1.117
20	0.335	0.503	1.500
21	4.820	2.867	1.681
22	0.417	0.531	1.275
23	0.488	0.517	1.061
24	5.678	4.320	1.314
25	1.280	1.92	1.525
26	6.487	3.375	1.922
27	0.122	0.216	1.767
28	0.230	0.225	1.023
29	10.380	6.106	1.700

30	0.365	0.249	1.466
31	3.367	4.654	1.382
32	1.330	1.036	1.284
33	0.371	0.354	1.049
34	0.497	0.298	1.665
35	0.186	0.234	1.257
36	0.400	0.374	1.069

Table 4. Seven candidate molecules from ADSC secretome

Uniprot_ID	Protein (Gene)
ANXA_HUMAN	Annexin A1 (ANXA1)
CFAH_HUMAN	Complement factor H (CFH)
DKK3_HUMAN	dickkopf WNT signaling pathway inhibitor 3 (DKK3)
LG3BP_HUMAN	Galectin 3 binding protein (LGALS3BP)
PTX3_HUMAN	Pentraxin 3 (PTX3)
PROS_HUMAN	Protein S (alpha) (PROS1)
PEDF_HUMAN	Serpin family F member 1 (SERPINF1)

12. PTX3 of ADSC secretome is a key molecule of regulating inflammatory activity of macrophage

To verify PTX3 and LGALS3BP as important factors for ADSC secretome, antibody neutralization was performed. Peritoneal macrophages were treated with 100 μg/ml ADSC secretome in the absence or presence of 1 μg/ml of neutralizing antibodies of PTX3 and LGALS3BP. PTX3 neutralizing antibody prevented mRNA expressions of iNOS and TNF-α by ADSC secretome from decreasing (Fig. 19A). Further, mRNA expressions of anti-inflammatory markers, Arg-1 and IL-10, were disturbed to the same level as the control by the PTX3 neutralizing antibody (Fig. 19B). Released cytokine levels were checked with cultured supernatant to confirm the effect of neutralization. Like the result of mRNA levels, decreased TNF-α and IL-1β by ADSC secretome were increased and increased IL-10 were decreased to the same level as the control by PTX3 neutralization antibody (Fig. 19C). By the way, LGALS3BP neutralization only affected IL-10 mRNA level (Fig 19B). Then, we tested the change in M2b/c markers by the neutralization. PTX3 neutralization abated the increase of LIGHT and MerTK mRNA levels by ADSC secretome (Fig. 20A). Nonetheless, only MerTK MFI was affected PTX3 neutralization not LIGHT MFI (Fig. 20B and 20C).

Recombinant PTX3 (rhPTX3) was treated to peritoneal macrophage to confirm the effect of PTX3. mRNA expressions of pro-inflammatory markers were decreased and of anti-inflammatory markers were increased by rhPTX3 (Fig. 21A and 21B) Also, mRNA levels of LIGHT and MerTK were increased by rhPTX3 (Fig. 21C). Taken together,

PTX3 rather than LGALS3BP is a main effector molecule of ADSC secretome in macrophage polarization.

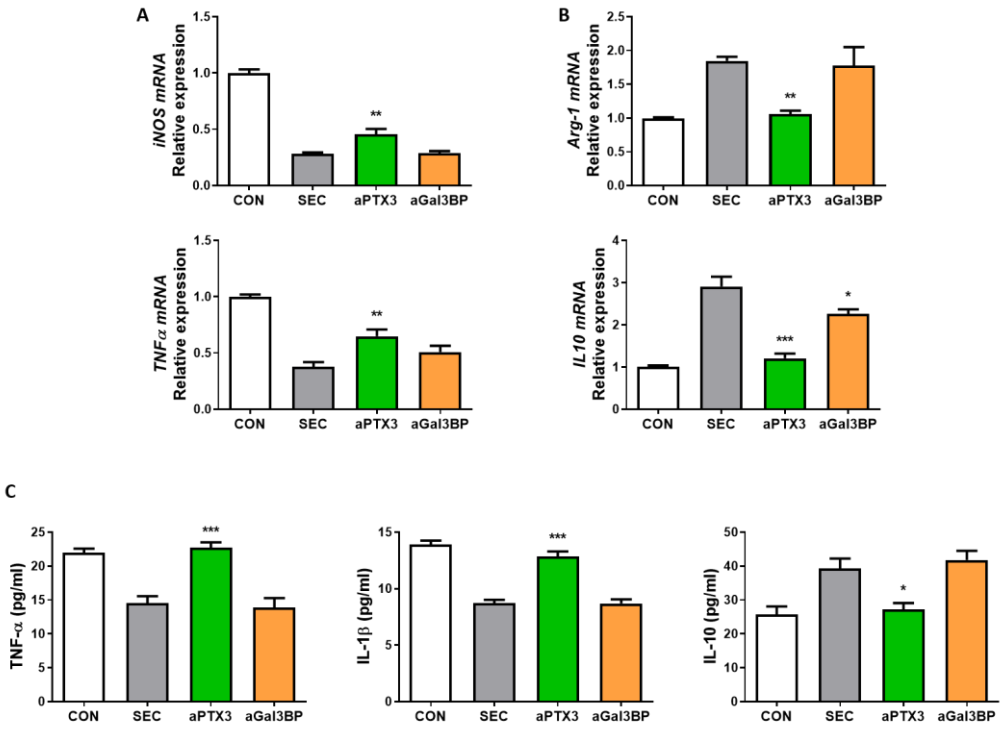

Figure 20. Weakening the effect in M2 polarization of ADSC secretome by blocking PTX3 and LGAL3BP. Peritoneal macrophages treated with 100 μg/ml ADSC secretome in the absence or presence of 1 μg/ml neutralizing antibodies of PTX3 and LGAL3BP. Quantification of (A) pro-inflammatory markers (iNOS and TNF-α) and (B) anti-inflammatory markers (Arg-1 and IL-10) mRNA levels by qRT-PCR. (C) Quantification of TNF-α, IL-1β, and IL-10 in culture supernatant. Data are expressed as mean ± SEM of three independent experiments. Statistical significance was determined by one-way ANOVA with a bonferroni post-test; $*P < 0.05$, $**P < 0.01$, $***P < 0.001$ compared to control group. SEC: ADSC secretome; aPTX3: anti-PTX3; aGal3BP: anti-LAGAL3BP.

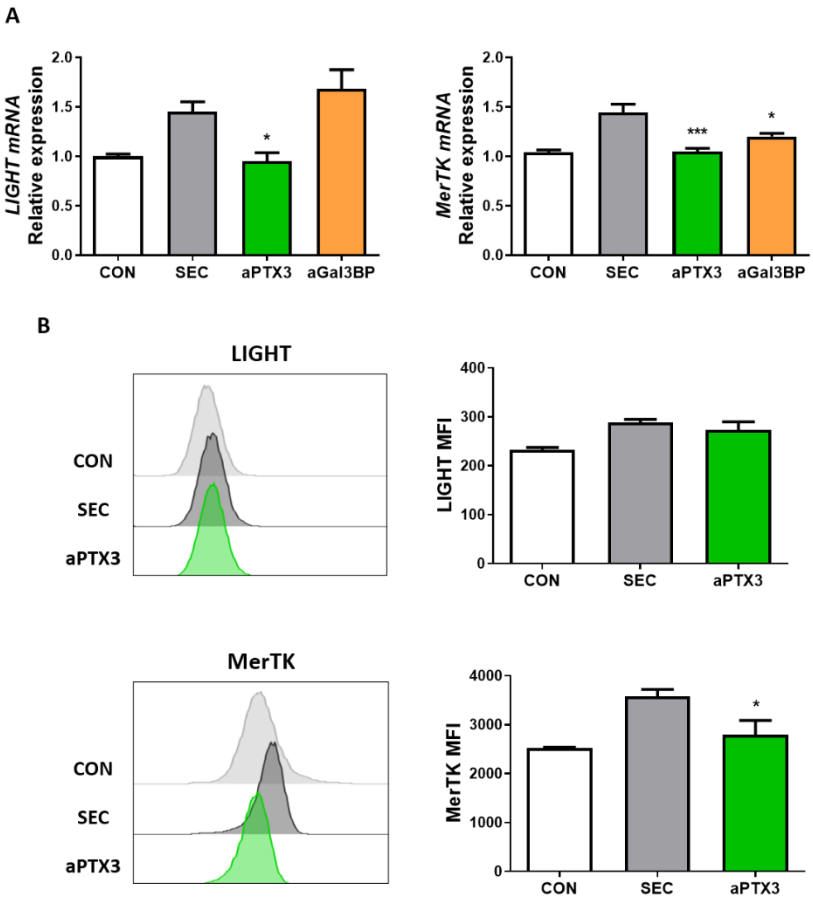

Figure 21. Weakening the effect in M2 subtype polarization of ADSC secretome by blocking PTX3 and LGAL3BP. Peritoneal macrophages treated with 100 μg/ml ADSC secretome in the absence or presence of 1μg/ml neutralizing antibodies of PTX3 and LGAL3BP. (A) Quantification of LIGHT and MerTK mRNA levels by qRT-PCR. (B) Flow cytometry analysis of LIGHT and MerTK in F4/80^{+} macrophages. Data are expressed as mean ± SEM of three independent experiments. Statistical significance was determined by one-way ANOVA with a bonferroni post-test; *$P < 0.05$, ***$P < 0.001$ compared to control group. CON: Control SEC: ADSC secretome; aPTX3: anti-PTX3; aGal3BP: anti-LAGAL3BP; MFI: Mean fluorescent intensity.

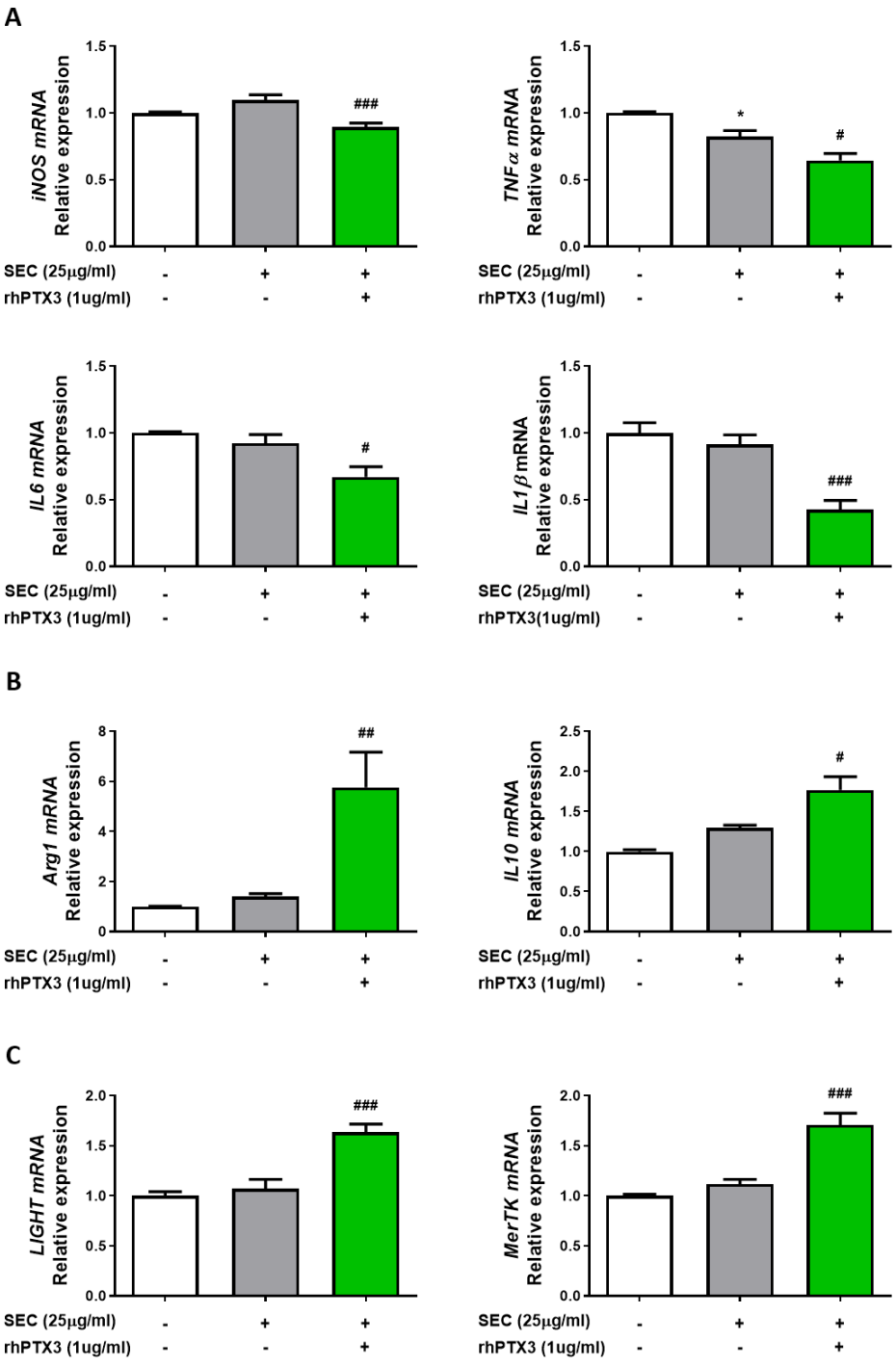

Figure 22. M2b/c polarization of peritoneal macrophage by PTX3 with ADSC secretome. Peritoneal macrophages treated with 25 μg/ml ADSC secretome in the absence or presence of 1 μg/ml recombinant PTX3 protein. Quantification of (A) pro-inflammatory markers (iNOS, TNF-α, IL-6, and IL-1β), (B) anti-inflammatory markers (Arg-1 and IL-10), and (C) M2b/c markers (LIGHT and MerTK) mRNA levels by qRT-PCR. Data are expressed as mean ± SEM of three independent experiments. Statistical significance was determined by one-way ANOVA with a bonferroni post-test; *P < 0.05 compared to control group and $^{\#}P < 0.05$, $^{\#\#}P < 0.01$, $^{\#\#\#}P < 0.001$ compared to ADSC secretome treatment group. SEC: ADSC secretome; rhPTX3: Recombinant human PTX3 protein.

IV. DISCUSSION

MSCs have been tried to be used as therapeutic agent to various inflammatory diseases due to their ability of regulating the immune response.[1] Not only cell-cell contact but also paracrine effect of MSCs gets attention as MSC transplantation has several limitations. MSC secretome is composed of extracellular vesicles, exosomes and microvesicles, and soluble factors, cytokines, chemokines, growth factors, and proteases.[39,40] Previous reports showed that paracrine effect of MSCs induce M2 polarization of macrophage and several soluble factors responsible for the effect were explored.[41] Despite the active studies, the mechanism of MSCs therapy still needs to be compensated. Therefore, we expanded MSC-macrophage interactions to exploring NF-κB/AKT and STAT/SOCS pathways of macrophage and PTX3 as active molecule inducing polarization of M2b/c like subtype.

With treatment of ADSC derived secretome to LPS stimulated RAW264.7 cell and peritoneal macrophage, M1 markers (CD197, CD86, TNF-α, and iNOS) were suppressed and M2 markers (Arg-1, CD206, and IL-10) were activated. Cyclooxygenase-2 (COX-2) and microsomal prostaglandin E synthase-1 (mPGES1) expression were decreased by ADSC derived secretome in same aspect. COX-2 and mPGES1 are in pathway of prostaglandin e2 (PGE2) production, closely involved in inflammation and immune disorders.[42] Jin et al. reported that MSC-CM decreased COX-2 expression of LPS activated macrophage.[43]

NF-κB/AKT pathway is one of the main signaling pathways of regulating inflammation. NF-κB is responsible for induction of inflammatory cytokines of macrophage and can be

developed by phosphorylated AKT.[44] ADSC secretome suppressed phosphorylation of NF-κB p65 and AKT and increased PTEN expression of LPS stimulated RAW264.7 cells. PTEN is an inhibitor of PI3K/AKT pathway as blocking phosphorylation of AKT by interference in formation of PI (3,4,5) P3 from PI (4,5) P2.[45] Increased PTEN expression and reduced AKT phosphorylation by ADSC secretome were confirmed with a PTEN inhibitor, SF1670, which diminished the regulating ability of ADSC secretome toward macrophage.

JAK/STAT pathway is the other important pathway in macrophage polarization. STAT1, induced representatively by IFN-γ, is mainly responsible for M1 polarization. STAT3 and STAT6 generate M2 phenotype and activated typically by IL-10 and IL-4, respectively.[46,47] SOCS1 is known for suppressing the STAT1 pathway and also NF-κB signaling,[48,49] so SOCS1, increased by ADSC secretome, might inhibit STAT1 phosphorylation in this study. ADSC secretome also increased STAT3 phosphorylation and SOCS3 expression. SOCS3 suppressed M1 phenotype by hindering IL-6R related STAT3 activation and is induced by IL-10 mediated STAT3 activation as a negative feedback.[48,50] As IL-10 is an inducer of and also produced by M2c macrophage, SOCS3 and STAT3 are also closely related to the M2c phenotype, which has functions as immuno-regulation and tissue remodeling.[51,52]

M2 subtype of macrophages is divided into M2a, M2b, and M2c mainly according to stimuli: IL-4 or IL-13 for M2a, stimulant of FCγ receptors with TLR stimulant for M2b, Glucocorticoid or IL-10 for M2c.[53] Each subtype is classified with particular marker and Ym-1 for M2a, SPHK1 and LIGHT for M2b, and MerTK for M2c were used to classify in

this study. Philipp et al. addressed that bone marrow derived MSC induce M2b polarization with increasing SPHK1 and LIGHT expressions[28] and Sun et al. demonstrated that adipose tissue derived MSC induce M2b/c polarization with increasing IL-10 and SPHK1 expressions.[29] When ADSC secretome was treated to peritoneal macrophage, only LIGHT and MerTK expressions were increased without LPS stimulation but expressions for every marker were increased with LPS stimulation. In the steady state condition, peritoneal macrophages were mostly comprised of large peritoneal macrophages, which function as apoptotic cell clearance, efferocytosis and tissue repair.[54] MerTK on macrophages is known for regulating the efferocytosis by binding Gas 6 or Protein S.[55,56] ADSC secretome might reinforce the efferocytosis of macrophage and control inflammation with increasing MerTK expression. M2b macrophages are known for regulatory macrophages, but they show shared some feature with M1 phenotype such as secreting TNF-α and IL-6. LIGHT and SPHK1, however, are used for distinguishing M2b macrophage from others.[21] Even though LIGHT is more favorable than SPHK1 to be used as M2b markers, both markers can be supported each other.[57] ADSC secretome might affect M2b polarization of peritoneal macrophage in the steady state incompletely as only LIGHT expression is increased, whereas peritoneal macrophage needs to be polarized to M2b phenotype completely with the stimulation to action as regulatory function.

Previous studies addressed PGE2, TSG-6, IL-6, and TGF-β1 as candidate molecules involved in polarization of macrophage and suppression of inflammation. Those reports, however, did not contain analysis of MSC secretome composition such as proteomics or

antibody array. Unlike previous reports, we performed LC/MS-MS proteomics analysis of ADSC secretome to verify composition and discovered 84 proteins as a result. 7 candidate molecules which contain secreted, immune response, and inflammation as a keyword of DAVID bioinformatics analysis were selected among 84 proteins. MSCs have a characteristic that the degree of function is different depending on the donor.[58] As we used this characteristic to identify active molecule of ADSC secretome, we analyzed three sets of secretome: two sets show similar function in suppression of CD86 expression, but one set show weak suppression of CD86 expression in peritoneal macrophage. Pentraxin-3 (PTX3), complement factor H (CFH) and galectin-3 binding protein (LGALS3BP) were selected based on image analysis that identify common spots between two sets of secretome with similar function and having 2-fold difference compared to one set of secretome with weak function.

PTX3, also named as TNF-inducible gene 14 (TSG-14), is one of the pattern recognition molecules (PRMs) and involved in inflammation, innate immunity, haemostasis, and tissue repair.[59,60] Shiraki et al reported that PTX3 restrained inflammatory markers, TNF-α, IL-1β, AKT phosphorylation, and nuclear NF-κB, of human macrophage cell line, THP-1 cells.[61] Additionally, Kim et al. reported that soluble PTX3 of human umbilical cord blood derived MSC decrease M1 marker expression and increase M2 marker expression of rat macrophage cell line, NR8383.[62] We confirmed that function of ADSC secretome was abated by PTX3 neutralizing antibody and PTX3 recombinant protein treatment with small amount of ADSC secretome induced M2-like polarization of

peritoneal macrophage. Moreover, PTX3 was involved in M2b/c like polarization of macrophage. The neutralizing antibody of PTX3 weakened MerTK expression, increased by ADSC secretome and recombinant PTX3 protein induced LIGHT and MerTK expression. Together, secreted PTX3 is a key molecule of ADSC secretome function in macrophage polarization.

One of the main limitations of MSC therapy is shortage of criteria for therapeutic efficacy.[4] Our study suggested that PTX3 can be used as a criterion for quality control of ADSC secretome. The amount of PTX3 secreted by MSC has donor-variable and ability of MSC depends on that.[62] Our image analysis also showed that specific ADSC secretome has high spot density of PTX3 and PTX3 functions as main effector of M2b/c-like polarization. Therefore, setting cut-off value with PTX3 might be helpful for future MSC treatment. Also, there are several priming methods to amplify the therapeutic effect of MSC such as addition of cytokines or culture in hypoxia conditions.[63] Previous reports reported that increased levels of PTX3 are observed at TNF-α, IL-1β, and IL-6 primed bone marrow-derived MSC and TNF-α primed adipose tissue derived MSC.[64,65] The way to amplify the PTX3 level should be confirmed and checking the effect of the priming MSC to macrophage polarization might be helpful.

V. CONCLUSION

In conclusion, ADSC secretome regulated inflammation in RAW264.7 cell via NF-κB/AKT and STAT signaling pathways with the increase of PTEN, SOCS1, and SOCS3. Also, in the animal models of RA and SLE, ADSC secretome treatment progress was observed with M2 polarization of peritoneal macrophages. Moreover, ADSC secretome induced M2b/c-like phenotype of peritoneal macrophages with escalating LIGHT and MerTK expressions. 84 proteins in ADSC secretome were identified through LC/MS-MS proteomics analysis. Neutralization assay and recombinant protein confirmed that PTX3 is a key molecule in secretome. This study indicates that ADSC secretome could replace the MSC cell therapy and establish the standard of therapeutic efficacy by applying PTX3 as a marker.

REFERENCES

1. Wei X, Yang X, Han ZP, Qu FF, Shao L, Shi YF. Mesenchymal stem cells: a new trend for cell therapy. Acta Pharmacol Sin 2013;34:747-54.
2. Mohamed-Ahmed S, Fristad I, Lie SA, Suliman S, Mustafa K, Vindenes H, et al. Adipose-derived and bone marrow mesenchymal stem cells: a donor-matched comparison. Stem Cell Res Ther 2018;9:168.
3. Volarevic V, Markovic BS, Gazdic M, Volarevic A, Jovicic N, Arsenijevic N, et al. Ethical and Safety Issues of Stem Cell-Based Therapy. Int J Med Sci 2018;15:36-45.
4. Bang OY, Kim EH, Cha JM, Moon GJ. Adult Stem Cell Therapy for Stroke: Challenges and Progress. J Stroke 2016;18:256-66.
5. Choumerianou DM, Dimitriou H, Kalmanti M. Stem cells: promises versus limitations. Tissue Eng Part B Rev 2008;14:53-60.
6. Spees JL, Lee RH, Gregory CA. Mechanisms of mesenchymal stem/stromal cell function. Stem Cell Res Ther 2016;7:125.
7. Gallina C, Turinetto V, Giachino C. A New Paradigm in Cardiac Regeneration: The Mesenchymal Stem Cell Secretome. Stem Cells Int 2015;2015:765846.
8. Vizoso FJ, Eiro N, Cid S, Schneider J, Perez-Fernandez R. Mesenchymal Stem Cell Secretome: Toward Cell-Free Therapeutic Strategies in Regenerative Medicine. Int J Mol Sci 2017;18.
9. Jasim SA, Yumashev AV, Abdelbasset WK, Margiana R, Markov A, Suksatan W, et al. Shining the light on clinical application of mesenchymal stem cell therapy in autoimmune diseases. Stem Cell Res Ther 2022;13:101.
10. Fugger L, Jensen LT, Rossjohn J. Challenges, Progress, and Prospects of Developing Therapies to Treat Autoimmune Diseases. Cell 2020;181:63-80.
11. Dazzi F, Krampera M. Mesenchymal stem cells and autoimmune diseases. Best Pract Res Clin Haematol 2011;24:49-57.
12. Sun L, Wang D, Liang J, Zhang H, Feng X, Wang H, et al. Umbilical cord

mesenchymal stem cell transplantation in severe and refractory systemic lupus erythematosus. Arthritis Rheum 2010;62:2467-75.

13. Park KH, Mun CH, Kang MI, Lee SW, Lee SK, Park YB. Treatment of Collagen-Induced Arthritis Using Immune Modulatory Properties of Human Mesenchymal Stem Cells. Cell Transplant 2016;25:1057-72.
14. Karussis D, Karageorgiou C, Vaknin-Dembinsky A, Gowda-Kurkalli B, Gomori JM, Kassis I, et al. Safety and Immunological Effects of Mesenchymal Stem Cell Transplantation in Patients With Multiple Sclerosis and Amyotrophic Lateral Sclerosis. Archives of neurology 2010;67.
15. Ovchinnikov DA. Macrophages in the embryo and beyond: much more than just giant phagocytes. Genesis 2008;46:447-62.
16. Murray PJ, Allen JE, Biswas SK, Fisher EA, Gilroy DW, Goerdt S, et al. Macrophage activation and polarization: nomenclature and experimental guidelines. Immunity 2014;41:14-20.
17. Martinez FO, Gordon S. The M1 and M2 paradigm of macrophage activation: time for reassessment. F1000Prime Rep 2014;6:13.
18. Mantovani A, Biswas SK, Galdiero MR, Sica A, Locati M. Macrophage plasticity and polarization in tissue repair and remodelling. J Pathol 2013;229:176-85.
19. Roszer T. Understanding the Mysterious M2 Macrophage through Activation Markers and Effector Mechanisms. Mediators Inflamm 2015;2015:816460.
20. Li P, Ma C, Li J, You S, Dang L, Wu J, et al. Proteomic characterization of four subtypes of M2 macrophages derived from human THP-1 cells. J Zhejiang Univ Sci B 2022;23:407-22.
21. Wang LX, Zhang SX, Wu HJ, Rong XL, Guo J. M2b macrophage polarization and its roles in diseases. J Leukoc Biol 2019;106:345-58.
22. Gensel JC, Zhang B. Macrophage activation and its role in repair and pathology after spinal cord injury. Brain Res 2015;1619:1-11.
23. Ahamada MM, Jia Y, Wu X. Macrophage Polarization and Plasticity in Systemic

Lupus Erythematosus. Front Immunol 2021;12:734008.

24. Yue Y, Yang X, Feng K, Wang L, Hou J, Mei B, et al. M2b macrophages reduce early reperfusion injury after myocardial ischemia in mice: A predominant role of inhibiting apoptosis via A20. Int J Cardiol 2017;245:228-35.
25. Li Y, Cai L, Wang H, Wu P, Gu W, Chen Y, et al. Pleiotropic regulation of macrophage polarization and tumorigenesis by formyl peptide receptor-2. Oncogene 2011;30:3887-99.
26. Alivernini S, MacDonald L, Elmesmari A, Finlay S, Tolusso B, Gigante MR, et al. Distinct synovial tissue macrophage subsets regulate inflammation and remission in rheumatoid arthritis. Nat Med 2020;26:1295-306.
27. Cho DI, Kim MR, Jeong HY, Jeong HC, Jeong MH, Yoon SH, et al. Mesenchymal stem cells reciprocally regulate the M1/M2 balance in mouse bone marrow-derived macrophages. Exp Mol Med 2014;46:e70.
28. Philipp D, Suhr L, Wahlers T, Choi YH, Paunel-Gorgulu A. Preconditioning of bone marrow-derived mesenchymal stem cells highly strengthens their potential to promote IL-6-dependent M2b polarization. Stem Cell Res Ther 2018;9:286.
29. Sun M, Sun L, Huang C, Chen BC, Zhou Z. Induction of Macrophage M2b/c Polarization by Adipose Tissue-Derived Mesenchymal Stem Cells. J Immunol Res 2019;2019:7059680.
30. Wang J, Liu Y, Ding H, Shi X, Ren H. Mesenchymal stem cell-secreted prostaglandin E(2) ameliorates acute liver failure via attenuation of cell death and regulation of macrophage polarization. Stem Cell Res Ther 2021;12:15.
31. Vasandan AB, Jahnavi S, Shashank C, Prasad P, Kumar A, Prasanna SJ. Human Mesenchymal stem cells program macrophage plasticity by altering their metabolic status via a PGE(2)-dependent mechanism. Sci Rep 2016;6:38308.
32. Song WJ, Li Q, Ryu MO, Ahn JO, Ha Bhang D, Chan Jung Y, et al. TSG-6 Secreted by Human Adipose Tissue-derived Mesenchymal Stem Cells Ameliorates DSS-induced colitis by Inducing M2 Macrophage Polarization in Mice. Sci Rep

2017;7:5187.

33. Liu F, Qiu H, Xue M, Zhang S, Zhang X, Xu J, et al. MSC-secreted TGF-beta regulates lipopolysaccharide-stimulated macrophage M2-like polarization via the Akt/FoxO1 pathway. Stem Cell Res Ther 2019;10:345.
34. Camps M, Ruckle T, Ji H, Ardissone V, Rintelen F, Shaw J, et al. Blockade of PI3Kgamma suppresses joint inflammation and damage in mouse models of rheumatoid arthritis. Nat Med 2005;11:936-43.
35. Kim AJ, Ro H, Kim H, Chang JH, Lee HH, Chung W, et al. Klotho and S100A8/A9 as Discriminative Markers between Pre-Renal and Intrinsic Acute Kidney Injury. PLoS One 2016;11:e0147255.
36. Huang da W, Sherman BT, Lempicki RA. Systematic and integrative analysis of large gene lists using DAVID bioinformatics resources. Nat Protoc 2009;4:44-57.
37. Liu T, Zhang L, Joo D, Sun SC. NF-kappaB signaling in inflammation. Signal Transduct Target Ther 2017;2:17023-.
38. Rao Z, Cao H, Shi B, Liu X, Luo J, Zeng N. Inhibitory Effect of Jing-Fang Powder n-Butanol Extract and Its Isolated Fraction D on Lipopolysaccharide-Induced Inflammation in RAW264.7 Cells. J Pharmacol Exp Ther 2019;370:62-71.
39. L PK, Kandoi S, Misra R, S V, K R, Verma RS. The mesenchymal stem cell secretome: A new paradigm towards cell-free therapeutic mode in regenerative medicine. Cytokine Growth Factor Rev 2019;46:1-9.
40. Sun DZ, Abelson B, Babbar P, Damaser MS. Harnessing the mesenchymal stem cell secretome for regenerative urology. Nat Rev Urol 2019;16:363-75.
41. Lu D, Xu Y, Liu Q, Zhang Q. Mesenchymal Stem Cell-Macrophage Crosstalk and Maintenance of Inflammatory Microenvironment Homeostasis. Front Cell Dev Biol 2021;9:681171.
42. Kawahara K, Hohjoh H, Inazumi T, Tsuchiya S, Sugimoto Y. Prostaglandin E2-induced inflammation: Relevance of prostaglandin E receptors. Biochim Biophys Acta 2015;1851:414-21.

43. Jin QH, Kim HK, Na JY, Jin C, Seon JK. Anti-inflammatory effects of mesenchymal stem cell-conditioned media inhibited macrophages activation in vitro. Sci Rep 2022;12:4754.
44. Dan HC, Cooper MJ, Cogswell PC, Duncan JA, Ting JP, Baldwin AS. Akt-dependent regulation of NF-kappaB is controlled by mTOR and Raptor in association with IKK. Genes Dev 2008;22:1490-500.
45. Vergadi E, Ieronymaki E, Lyroni K, Vaporidi K, Tsatsanis C. Akt Signaling Pathway in Macrophage Activation and M1/M2 Polarization. J Immunol 2017;198:1006-14.
46. Malyshev I, Malyshev Y. Current Concept and Update of the Macrophage Plasticity Concept: Intracellular Mechanisms of Reprogramming and M3 Macrophage "Switch" Phenotype. Biomed Res Int 2015;2015:341308.
47. Wilson HM. SOCS Proteins in Macrophage Polarization and Function. Front Immunol 2014;5:357.
48. Yoshimura A, Naka T, Kubo M. SOCS proteins, cytokine signalling and immune regulation. Nat Rev Immunol 2007;7:454-65.
49. Ryo A, Suizu F, Yoshida Y, Perrem K, Liou YC, Wulf G, et al. Regulation of NF-kappaB signaling by Pin1-dependent prolyl isomerization and ubiquitin-mediated proteolysis of p65/RelA. Mol Cell 2003;12:1413-26.
50. Cevey AC, Penas FN, Alba Soto CD, Mirkin GA, Goren NB. IL-10/STAT3/SOCS3 Axis Is Involved in the Anti-inflammatory Effect of Benznidazole. Front Immunol 2019;10:1267.
51. Koscso B, Csoka B, Kokai E, Nemeth ZH, Pacher P, Virag L, et al. Adenosine augments IL-10-induced STAT3 signaling in M2c macrophages. J Leukoc Biol 2013;94:1309-15.
52. Miki S, Suzuki JI, Takashima M, Ishida M, Kokubo H, Yoshizumi M. S-1-Propenylcysteine promotes IL-10-induced M2c macrophage polarization through prolonged activation of IL-10R/STAT3 signaling. Sci Rep 2021;11:22469.

53. Martinez FO, Sica A, Mantovani A, Locati M. Macrophage activation and polarization. Front Biosci 2008;13:453-61.
54. Cassado Ados A, D'Imperio Lima MR, Bortoluci KR. Revisiting mouse peritoneal macrophages: heterogeneity, development, and function. Front Immunol 2015;6:225.
55. Myers KV, Amend SR, Pienta KJ. Targeting Tyro3, Axl and MerTK (TAM receptors): implications for macrophages in the tumor microenvironment. Mol Cancer 2019;18:94.
56. Jimenez-Garcia L, Mayer C, Burrola PG, Huang Y, Shokhirev MN, Lemke G. The TAM receptor tyrosine kinases Axl and Mer drive the maintenance of highly phagocytic macrophages. Front Immunol 2022;13:960401.
57. Zhang Q, Sioud M. Tumor-Associated Macrophage Subsets: Shaping Polarization and Targeting. Int J Mol Sci 2023;24.
58. Stroncek DF, Jin P, McKenna DH, Takanashi M, Fontaine MJ, Pati S, et al. Human Mesenchymal Stromal Cell (MSC) Characteristics Vary Among Laboratories When Manufactured From the Same Source Material: A Report by the Cellular Therapy Team of the Biomedical Excellence for Safer Transfusion (BEST) Collaborative. Front Cell Dev Biol 2020;8:458.
59. Doni A, Stravalaci M, Inforzato A, Magrini E, Mantovani A, Garlanda C, et al. The Long Pentraxin PTX3 as a Link Between Innate Immunity, Tissue Remodeling, and Cancer. Front Immunol 2019;10:712.
60. Porte R, Davoudian S, Asgari F, Parente R, Mantovani A, Garlanda C, et al. The Long Pentraxin PTX3 as a Humoral Innate Immunity Functional Player and Biomarker of Infections and Sepsis. Front Immunol 2019;10:794.
61. Shiraki A, Kotooka N, Komoda H, Hirase T, Oyama JI, Node K. Pentraxin-3 regulates the inflammatory activity of macrophages. Biochem Biophys Rep 2016;5:290-5.
62. Kim M, Kwon JH, Bae YK, Kim GH, Um S, Ha J, et al. Soluble PTX3 of Human

Umbilical Cord Blood-Derived Mesenchymal Stem Cells Attenuates Hyperoxic Lung Injury by Activating Macrophage Polarization in Neonatal Rat Model. Stem Cells Int 2020;2020:1802976.

63. Noronha NC, Mizukami A, Caliari-Oliveira C, Cominal JG, Rocha JLM, Covas DT, et al. Priming approaches to improve the efficacy of mesenchymal stromal cell-based therapies. Stem Cell Res Ther 2019;10:131.

64. Maffioli E, Nonnis S, Angioni R, Santagata F, Cali B, Zanotti L, et al. Proteomic analysis of the secretome of human bone marrow-derived mesenchymal stem cells primed by pro-inflammatory cytokines. J Proteomics 2017;166:115-26.

65. Lee MJ, Kim J, Kim MY, Bae Y-S, Ryu SH, Lee TG, et al. Proteomic Analysis of Tumor Necrosis Factor-α-Induced Secretome of Human Adipose Tissue-Derived Mesenchymal Stem Cells. Journal of Proteome Research 2010;9:1754-62.

ABSTRACT(IN KOREAN)

류마티스 관절염 및 전신홍반루푸스 마우스 모델에서 중간엽 줄기세포 유래 분비단백체의 면역조절 메커니즘 규명

<지도교수 박 용 범>

연세대학교 대학원 의과학과

윤 태 준

중간엽 줄기세포는 면역조절 능력과 항염증 능력을 다양한 질병들과 면역세포들에 나타낸다. 하지만 그들은 치료제재로서의 한계들을 가지고 있다. 중간엽 줄기세포에서 분비되는 생체 활성 물질들인 분비 인자는 중간엽 줄기세포의 이러한 한계들을 극복하기 위한 대체재로써 제안되고 있다. 면역체계의 결함으로 발생되는 자가면역 질환들은 중간엽 줄기세포를 미충족 수요를 해결하기 위한 새로운 치료제로 적용하려는 질병들 중 하나이다. 대식세포들은 면역체계를 조절함으로 항상성에 역할을 수행하며 염증성 환경을 조성하는 M1과 항염증성 환경을 조성하는 M2 두가지 기능적 표현형을 나타낸다. 최근, 대

식세포의 자세한 메커니즘을 위하여 M2a, M2b, M2c, M2d로 나타나는 M2 아류형들의 중요도가 부각되고 있다. 최근 논문들에서 중간엽 줄기세포의 치료 효능과 이에 대한 메커니즘을 밝혀내기 위하여 노력하고 있지만, 여전히 이에 대한 이해도는 부족하다. 본 연구에서는 중간엽 줄기세포 유래 분비 인자의 치료 효능을 연구하였고 분비 인자들 중 면역 조절의 물질들을 발굴하며 이에 대한 메커니즘을 확인하였다.

In vitro 실험들을 위하여 대식세포 세포주인, RAW264.7 세포와 복강 내 대식세포들을 LPS 자극의 유무 하에 지방 유래 중간엽 줄기세포 분비 인자로 처치하였다. 대식세포의 염증성 마커들과 항염증성 마커들을 유세포분석, qRT-PCR, 그리고 효소면역분석법으로 분석을 하였다. 중간엽 줄기세포 분비 인자들의 메커니즘을 밝혀내기 위하여 NF-κB/AKT and STAT/SOCS 신호 전달 경로를 웨스턴 블롯을 통하여 확인하였다. 중간엽 줄기세포 분비 인자의 치료 효능은 류마티스 관절염의 동물 모델인 콜라겐 유도성 관절염 동물과 전신홍반루푸스의 동물 모델인 NZB W/F1 마우스를 사용하여 확인하였다. 중간엽 줄기세포 분비 인자는 LC/MS-MS 프로테오믹스와 DAVID bioinformatics를 통하여 분석하였다. 중화 항체와 재조합단백질을 사용하여 중간엽 줄기세포 분비 인자 내의 주요 인자를 확인하였다.

중간엽 줄기세포 분비 인자는 대식세포의 iNOS와 TNF-α와 같은 염증성 마커들을 감소시키고 Arg-1과 IL-10과 같은 항염증성 마커들을 증가시켰다.

또한 중간엽 줄기세포 분비 인자는 대식세포의 PTEN의 발현을 증가시키고 NF-κB와 AKT의 인산화를 감소시켰으며 PTEN 억제재가 중간엽 줄기세포 분비 인자의 면역조절 효과를 감소시켰다. 중간엽 줄기세포 분비 인자에 의하여 SOCS1 과 SOCS3의 활성화 되었으며 STAT1의 인산화가 감소하고 STAT3의 인산화가 증가하였다. 중간엽 줄기세포 분비 인자는 CIA와 NZB/WF1 마우스의 질병 활성도를 감소시켰고 대식세포를 M2b/c-like 표현형으로 변화 시켰다. Proteomics 분석을 통하여 중간엽 줄기세포 분비인자들에서 84개의 단백체들을 확인하였고 그 중 7개의 후보 물질들(ANAX1, CFH, DKK3, LGALS3BP, PTX3, PROS1, and SERPINF1)을 선정하였다. 후보 물질들 중 PTX3를 선정하여 추가로 실험을 진행하였다. PTX3의 중화 항체는 중간엽 줄기세포 분비 인자의 기능을 약화시켰으며 재조합형 PTX3는 중간엽 줄기세포 분비 인자와 비슷한 효과를 나타냈다.

중간엽 줄기세포 분비 인자는 RAW264.7 세포와 류마티스 관절염과 정신홍반루푸스의 동물모델에서 염증을 조절하였다. 또한, 중간엽 줄기세포 분비 인자는 복강 내 대식세포의 M2b/c 분극화에 관여하며 PTX3가 이 효과에 주요 물질임을 확인하였다.

핵심되는 말 : 중간엽 줄기세포, 분비 인자, 대식세포, 자가면역질환, 면역조절

PUBLICATION LIST

1. Song JH*, **Yoon T***, Lee SM*, Mun CH, Kim D, Han J, et al. GeTe Nanosheets as Theranostic Agents for Multimodal Imaging and Therapy of Inflammatory Bowel Disease. Advanced Functional Materials 2021;32.
2. Ko E, **Yoon T**, Lee Y, Kim J, Park Y-B. ADSC secretome constrains NK cell activity by attenuating IL-2-mediated JAK-STAT and AKT signaling pathway via upregulation of CIS and DUSP4. Stem Cell Res Ther 2023;14:329.
3. Seo Y, Mun CH, Park SH, Jeon D, Kim SJ, **Yoon T**, et al. Punicalagin Ameliorates Lupus Nephritis via Inhibition of PAR2. Int J Mol Sci 2020;21.
4. Mun CH, Kim JO, Ahn SS, **Yoon T**, Kim SJ, Ko E, et al. Atializumab, a humanized anti-aminoacyl-tRNA synthetase-interacting multifunctional protein-1 (AIMP1) antibody significantly improves nephritis in (NZB/NZW) F1 mice. Biomaterials 2019;220:119408.
5. **Yoon T*** Ahn SS*, Ko E, Song JJ, Park YB, Lee SW. IL-6 Receptor Expression on the Surface of T Cells and Serum Soluble IL-6 Receptor Levels in Patients with Microscopic Polyangiitis and Granulomatosis with Polyangiitis. Journal of Clinical Medicine 2023;12.
6. Lee SJ*, **Yoon T***, Ha JW, Kim J, Lee KH, Lee JA, et al. Prevalence, clinical significance, and persistence of autoantibodies in COVID-19. Virol J 2023;20:236.
7. **Yoon T***, Ha JW*, Pyo JY, Song JJ, Park YB, Ahn SS, et al. Soluble triggering receptor expressed on myeloid cell-1 reflects the cross-sectional activity of microscopic polyangiitis and granulomatosis with polyangiitis. Heliyon 2023;9:e20881.
8. Lee TG*, **Yoon T***, Ko E, Pyo JY, Ahn SS, Song JJ, et al. Soluble Tyro-3 and Axl may reflect the current activity and renal involvement in patients with microscopic polyangiitis and granulomatosis with polyangiitis. Clin Exp Rheumatol 2023;41:948-55.
9. **Yoon T***, Pyo JY*, Ahn SS, Song JJ, Park YB, Lee SW. Serum soluble interleukin-

7 receptor alpha levels are negatively correlated with the simultaneous activity of antineutrophil cytoplasmic antibody-associated vasculitis. Clin Exp Rheumatol 2023;41:879-86.

10. Pyo JY*, **Yoon T***, Ahn SS, Song JJ, Park YB, Lee SW. Soluble immune checkpoint molecules in patients with antineutrophil cytoplasmic antibody-associated vasculitis. Sci Rep 2022;12:21319.
11. Ahn SS*, **Yoon T***, Song JJ, Park YB, Lee SW. Serum albumin, prealbumin, and ischemia-modified albumin levels in patients with ANCA-associated vasculitis: A prospective cohort study. PLoS One 2022;17:e0271055.
12. **Yoon T***, Ahn SS*, Pyo JY, Lee LE, Song JJ, Park YB, et al. Serum galectin-9 could be a potential biomarker in assessing the disease activity of antineutrophil cytoplasmic antibody-associated vasculitis. Clin Exp Rheumatol 2022;40:779-86.
13. **Yoon T***, Ahn SS*, Pyo JY, Lee LE, Song JJ, Park YB, et al. Correlation between serum cysteine-rich protein 61 and disease activity of antineutrophil cytoplasmic antibody-associated vasculitis. Clin Rheumatol 2021;40:3703-10.
14. **Yoon T***, Ahn SS*, Pyo JY, Lee LE, Song JJ, Park YB, et al. Predictive Ability of Serum IL-27 Level for Assessing Activity of Antineutrophil Cytoplasmic Antibody-Associated Vasculitis. Mediators Inflamm 2021;2021:6668884.
15. Ahn SS*, **Yoon T***, Song JJ, Park YB, Lee SW. Serum adipokine profiles in patients with microscopic polyangiitis and granulomatosis with polyangiitis: An exploratory analysis. PLoS One 2021;16:e0254226.
16. **Yoon T***, Ahn SS*, Pyo JY, Song JJ, Park YB, Lee SW. Association between follistatin-related protein 1 and the functional status of patients with anti-neutrophil cytoplasmic antibody-associated vasculitis. Chin Med J (Engl) 2021;134:1168-74.
17. Ahn SS*, **Yoon T***, Park YB, Prendecki M, Bhangal G, McAdoo SP, et al. Serum chitinase-3-like 1 protein is a useful biomarker to assess disease activity in ANCA-associated vasculitis: an observational study. Arthritis Res Ther 2021;23:77.
18. **Yoon T***, Ahn SS*, Yoo J, Song JJ, Park YB, Lee SW. Serum Amyloid A Is a

Biomarker of Disease Activity and Health-Related Quality-of-Life in Patients with Antineutrophil Cytoplasmic Antibody-Associated Vasculitis. Dis Markers 2020;2020:8847306.

19. **Yoon T***, Pyo JY*, Ahn SS, Song JJ, Park YB, Lee SW. Serum interleukin-16 significantly correlates with the Vasculitis Damage Index in antineutrophil cytoplasmic antibody-associated vasculitis. Arthritis Res Ther 2020;22:73.
20. **Yoon T***, Ahn SS*, Song JJ, Park YB, Lee SW. Serum interleukin-21 positivity could indicate the current activity of antineutrophil cytoplasmic antibody-associated vasculitis: a monocentric prospective study. Clin Rheumatol 2019;38:1685-90.
21. **Yoon T***, Ahn SS*, Jung SM, Song JJ, Park YB, Lee SW. Serum soluble programmed cell death protein 1 could predict the current activity and severity of antineutrophil cytoplasmic antibody-associated vasculitis: a monocentric prospective study. Clin Exp Rheumatol 2019;117:116-21.

*** Co-first author**